
I²EBench: A Comprehensive Benchmark for Instruction-based Image Editing

Yiwei Ma Jiayi Ji Ke Ye Weihuang Lin Zhibin Wang
Yonghan Zheng Qiang Zhou Xiaoshuai Sun Rongrong Ji
yiweima@stu.xmu.edu.cn xssun@xmu.edu.cn

Abstract

Significant progress has been made in the field of Instruction-based Image Editing (IIE). However, evaluating these models poses a significant challenge. A crucial requirement in this field is the establishment of a comprehensive evaluation benchmark for accurately assessing editing results and providing valuable insights for its further development. In response to this need, we propose **I²EBench**, a comprehensive benchmark designed to automatically evaluate the quality of edited images produced by IIE models from multiple dimensions. I²EBench consists of 2,000+ images for editing, along with 4,000+ corresponding original and diverse instructions. It offers three distinctive characteristics: 1) *Comprehensive Evaluation Dimensions*: I²EBench comprises 16 evaluation dimensions that cover both high-level and low-level aspects, providing a comprehensive assessment of each IIE model. 2) *Human Perception Alignment*: To ensure the alignment of our benchmark with human perception, we conducted an extensive user study for each evaluation dimension. 3) *Valuable Research Insights*: By analyzing the advantages and disadvantages of existing IIE models across the 16 dimensions, we offer valuable research insights to guide future development in the field. We will open-source I²EBench, including all instructions, input images, human annotations, edited images from all evaluated methods, and a simple script for evaluating the results from new IIE models. The code, dataset and generated images from all IIE models are provided in github: <https://github.com/cocoshe/I2EBench>.

1 Introduction

Instruction-based Image Editing (IIE) Brooks et al. [2023], Geng et al. [2023], Zhang et al. [2024a], Li et al. [2023e], Wang et al. [2023b], Zhang et al. [2023a], Fu et al. [2024], which aims to edit an image using a text instruction, provides a user-friendly way for the community to edit images. Over the past few years, significant progress has been made in IIE, with the development of diffusion models Ho et al. [2020], Sohl-Dickstein et al. [2015], Welling and Teh [2011], Kulikov et al. [2023] and large vision-language models (LVLMs) Radford et al. [2021], Li et al. [2022, 2023c], Xu et al. [2023], Liu et al. [2024, 2023a,b]. However, there is a pressing need for a comprehensive benchmark to effectively assess the performance of these models. An ideal evaluation framework should not only measure the editing quality across different dimensions but also align with human perception to ensure reliable measurements. Furthermore, the evaluation should highlight the specific strengths and weaknesses of each model, thereby offering valuable insights for future endeavors in data selection, training strategy selection, and architecture design within this field. However, evaluating an IIE model poses challenges due to the diverse range of editing types and the inherent difficulty in assessing the level of alignment between edited images and given instructions.

Existing evaluation metrics for IIE could be divided into three categories: 1) conventional metric; 2) user study; 3) benchmark. The first category Brooks et al. [2023], Geng et al. [2023], Zhang et al.

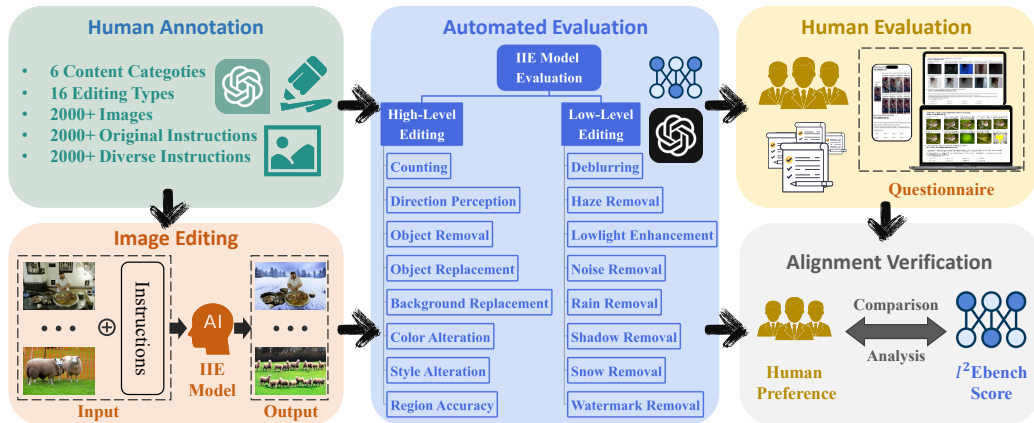


Figure 1: Overview of I²EBench, an automated system for evaluating the quality of editing results generated by instruction-based image editing (IIE) models. We collected a dataset of over 2000+ images from public datasets Lin et al. [2014], Guo et al. [2023b], Martin et al. [2001], Chen et al. [2021], Ancuti et al. [2019], Liu et al. [2021b,a], Qu et al. [2017], Nah et al. [2017], Shen et al. [2019], Wei et al. [2018] and annotated them with corresponding original editing instructions. To diversify the instructions, we used ChatGPT Achiam et al. [2023] to generate varied versions. With the collected images and the original/diverse editing instructions, we utilized existing IIE models to generate edited images. Subsequently, we developed an evaluation methodology to automatically assess the adherence of edited images to the provided instructions under different dimensions. We also implemented human evaluation to obtain human preferences for editing results of different IIE models. Finally, we analyzed the correlation between automated evaluation and human evaluation, confirming alignment with human perception.

[2024a], Li et al. [2023e], Wang et al. [2023b], Huang et al. [2024b] employs conventional metrics to evaluate IIE models, including CLIP Score Radford et al. [2021], CLIP Text-Image Direction Similarity Radford et al. [2021], PSNR Korhonen and You [2012], SSIM Wang et al. [2004], and LPIPS Zhang et al. [2018]. The advantage of this approach is its ease of use. However, a single metric is not suitable for evaluating all types of editing. For instance, CLIP score measures the similarity between images and text, making it less suitable for low-level visual editing tasks like denoising and low-light enhancement. Similarly, PSNR, which measures image similarity, is not adequate for high-level visual editing tasks such as object removal and replacement. The second category Li et al. [2023e], Zhang et al. [2023a], Fu et al. [2024] involves methods that evaluate the effectiveness of different techniques by soliciting ratings from human participants. This approach directly reflects human preferences and aligns the results with human perception. However, it is a costly method and lacks reproducibility, as the test sets and participants may be not consistent in each evaluation. The final category comprises benchmarks Kawar et al. [2023], Wang et al. [2023c], Basu et al. [2023], Huang et al. [2024a] specifically designed for evaluating IIE models. While these benchmarks are tailored for IIE, they have certain limitations. For example, TedBench Kawar et al. [2023] evaluates only 100 images with commonly occurring editing types, which may not sufficiently demonstrate the capabilities of IIE models. EditBench Wang et al. [2023c] focuses on mask-guided editing, rendering it unsuitable for evaluating mask-free methods. In EditVal Basu et al. [2023], only a limited set of dimensions related to size or location can be automatically evaluated, limiting its universality.

In this paper, we propose I²EBench, a comprehensive benchmark designed to automatically evaluate the performance of IIE models. I²EBench exhibits three attractive characteristics: 1) Comprehensive Evaluation Dimension, 2) Human Perception Alignment, and 3) Valuable Research Insights.

First and foremost, I²EBench offers a comprehensive evaluation dimension. These dimensions are categorized into two main types: *High-level Editing* and *Low-level Editing*. High-level editing primarily focuses on understanding instructions or editing specific areas of images, whereas low-level editing is more concerned with editing image details or the entire image. As shown in Fig. 1, both high-level and low-level editing consist of 8 fine-grained editing dimensions, which serve to demonstrate the model’s proficiency in high-level and low-level editing. We meticulously collected

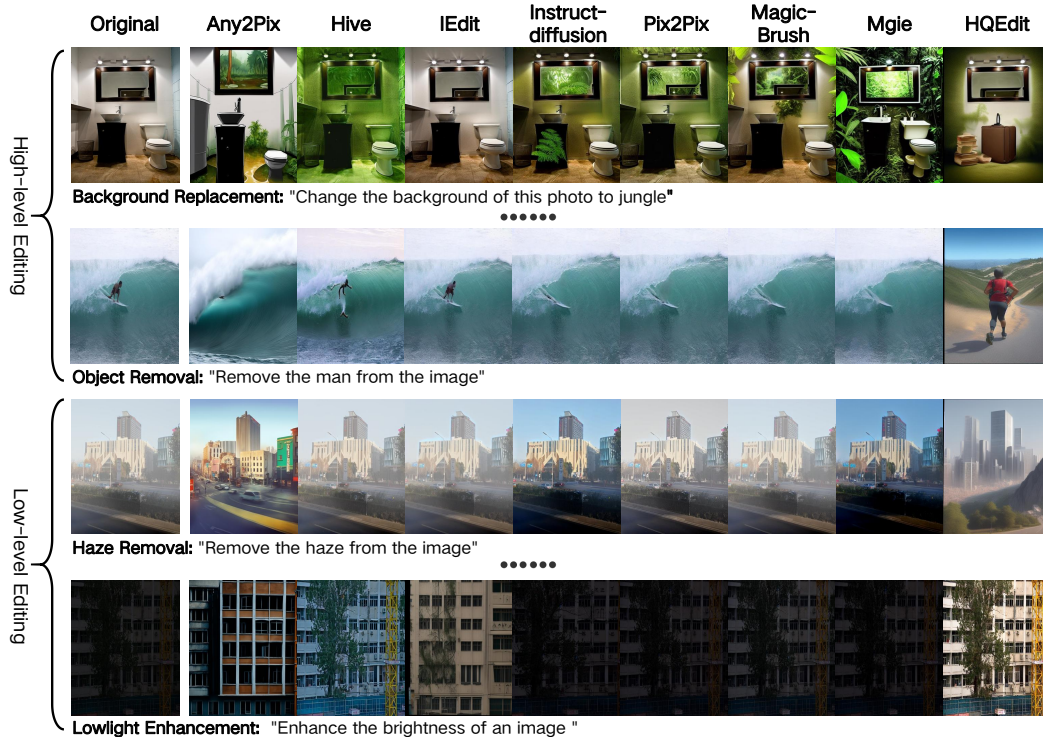


Figure 2: Visualization of the editing results on the proposed 16 evaluation dimensions using different IIE models, including InstructAny2Pix [Li et al. \[2023e\]](#), HIVE [Zhang et al. \[2023a\]](#), InstructEdit [Wang et al. \[2023b\]](#), InstructDiffusion [Geng et al. \[2023\]](#), InstructPix2Pix [Brooks et al. \[2023\]](#), MagicBrush [Zhang et al. \[2024a\]](#), MGIE [Fu et al. \[2024\]](#), and HQEdit [Hui et al. \[2024\]](#). A detailed version can be found in supplementary materials.

approximately 140 images for each editing dimension and annotated each image with an original editing text instruction. To diversify the instructions, we also utilized ChatGPT [Achiam et al. \[2023\]](#) to enhance the description of the instructions and obtain a wider range of variations. In addition to the multi-dimensional evaluation, we also conducted a multi-category evaluation to assess the model’s performance on different content categories. To achieve this, we included additional annotations for each instruction with different categories such as Animal, Object, Scenery, Plant, Human, and Global.

Second, the $I^2EBench$ score aligns with human perception. This is accomplished by collecting scores from human annotators for the outputs generated by different IIE models, covering multiple evaluation dimensions. By conducting a comprehensive analysis of both the $I^2EBench$ scores and the human scores, we have identified a substantial correlation between them. This discovery serves as compelling evidence, affirming that our proposed evaluation approach closely aligns with human perception.

Lastly, $I^2EBench$ offers valuable research insights through its systematic evaluation across various dimensions and categories. The proposed $I^2EBench$ not only facilitates a comprehensive assessment of existing models but also derives valuable insights into their respective strengths and weaknesses. These insights act as a roadmap for enhancing architecture design, refining data selection strategies, and ultimately elevating the quality of editing outcomes.

We are open-sourcing $I^2EBench$, including all instructions, input images, human annotations, edited images from all evaluated methods (like Fig. 2), and a simple script for evaluating the results of new IIE models. By making these resources freely available, we aim to foster fair comparisons within the field and facilitate valuable insights for community development.

2 Related Work

2.1 Instruction-based Image Editing

With the advancements in Generative Adversarial Networks (GAN) [Goodfellow et al. \[2014, 2020\]](#), [Mao et al. \[2017\]](#), [Karras et al. \[2019\]](#), [Yoon et al. \[2019\]](#), [Karras et al. \[2020a\]](#), [Chen et al. \[2018\]](#), [Zhang et al. \[2019\]](#) and Diffusion models [Song et al. \[2020\]](#), [Ho et al. \[2020\]](#), [Nichol and Dhariwal \[2021\]](#), [Kawar et al. \[2022\]](#), [Austin et al. \[2021\]](#), [Dockhorn et al. \[2022\]](#), text-to-image models [Saharia et al. \[2022\]](#), [Rombach et al. \[2022\]](#), [Ramesh et al. \[2021, 2022\]](#), [Betker et al. \[2023\]](#), [Karras et al. \[2019, 2020b\]](#) have made remarkable progress in recent years. As the demand for image editing continues to grow, a multitude of text-based image editing [Xu et al. \[2024\]](#), [Kawar et al. \[2023\]](#), [Zhang et al. \[2023b\]](#), [Saund et al. \[2003\]](#), [Zhang et al. \[2024b\]](#) models have emerged. One editing task, known as Prompt-based Image Editing (PIE) [Avrahami et al. \[2022\]](#), [Valevski et al. \[2023\]](#), [Hertz et al. \[2022\]](#), [Dong et al. \[2023\]](#), requires users to provide a target description along with the original image. The PIE model then analyzes the target description to modify the input image accordingly, generating a target image that matches the provided description. However, despite the lowered threshold for image editing, the requirement of describing the entire content of the target image in the description still poses challenges in terms of user interaction. To address this limitation, Instruction-based Image Editing (IIE) [Brooks et al. \[2023\]](#), [Geng et al. \[2023\]](#), [Li et al. \[2023e\]](#), [Fu et al. \[2024\]](#), [Huang et al. \[2024b\]](#) was proposed, which simplifies the user’s role to providing the original image and modification instructions (e.g., ‘Remove the dog’). One notable implementation, InstructPix2Pix [Brooks et al. \[2023\]](#), introduces a large-scale dataset for instruction-based image editing. The dataset is created using a fine-tuned GPT-3 [Brown et al. \[2020\]](#) and image pairs generated by the Prompt-to-Prompt diffusion model [Hertz et al. \[2022\]](#). Additionally, InstructPix2Pix proposes an instruction-based diffusion model for image editing based on this dataset. However, due to the automatic generation and filtering of the InstructPix2Pix dataset, concerns arise regarding its quality and potential noise. To address this, MagicBrush [Zhang et al. \[2024a\]](#) proposes a manually-annotated instruction-guided image editing dataset. In addition to textual instructions, InstructAny2Pix [Li et al. \[2023e\]](#) proposes a model that utilizes other modalities, such as audio and image, as instructions. To enhance the level of detail in instructions and improve the accuracy of editing results, MGIE [Fu et al. \[2024\]](#) introduces the use of Multimodal Large Language Models (MLLM) [Liu et al. \[2023a\]](#). SmartEdit [Achiam et al. \[2023\]](#), aiming to improve the editing capabilities of IIE models in complex scenes, incorporates MLLM into the IIE model to better comprehend instructions. Despite significant progress, evaluating the editing performance of IIE models remains a crucial concern. Therefore, in this paper, we present I²EBench, a systematic evaluation framework for these models. Our work includes an in-depth analysis of their strengths and weaknesses, offering valuable insights for the future development of IIE models.

2.2 Text-based Image Editing Benchmark

While numerous benchmarks [Marino et al. \[2019\]](#), [Hudson and Manning \[2019\]](#), [Bigham et al. \[2010\]](#), [Lu et al. \[2022\]](#), [Li et al. \[2023f,a,d\]](#), [Yu et al. \[2023\]](#), [Wu et al. \[2023b\]](#) have been introduced for evaluating vision-language tasks [Alayrac et al. \[2022\]](#), [Li et al. \[2023b\]](#), [Ye et al. \[2023\]](#), [Wu et al. \[2023a\]](#), [Dai et al. \[2024\]](#), [Hu et al. \[2024\]](#), the evaluation of text-based image editing models often relies on metrics such as CLIP Score [Radford et al. \[2021\]](#), PSNR [Korhonen and You \[2012\]](#), SSIM [Wang et al. \[2004\]](#), and LPIPS [Zhang et al. \[2018\]](#). Several existing studies have introduced benchmarks to assess the performance of image editing models. TedBench [Kawar et al. \[2023\]](#) presents a relatively small benchmark consisting of only 100 images and a limited set of highly common editing types. EditBench [Wang et al. \[2023c\]](#) is specifically designed to evaluate mask-guided image editing methods, which necessitate the availability of additional masks indicating the areas to be edited. In EditVal [Basu et al. \[2023\]](#), the evaluation of certain dimensions relies on manual labor, thereby limiting the reproducibility of performance. Moreover, the remaining dimensions primarily involve modifications to object size or position, lacking comprehensive coverage. While MagicBrush [Zhang et al. \[2024a\]](#) and Emu Edit [Sheynin et al. \[2023\]](#) propose test sets for evaluating editing performance, they still rely on conventional metrics such as L1, L2, CLIP-I, DINO, and CLIP-T, which may not accurately capture the nuances of all editing types. SmartEdit [Huang et al. \[2024b\]](#) specifically develops a benchmark tailored for complex editing scenarios, but it does not accommodate other editing scenarios. Considering the current absence of a systematic benchmark

that comprehensively evaluates the editing performance of IIE models across different editing types, we propose I²EBench to address this gap.

3 I²EBench

This section provides an overview of the main components of I²EBench. In Sec. 3.1, we provide a concise introduction to the principles, definitions, and evaluation methods of 16 dimensions. Sec. 3.2 outlines the process of data annotation. Lastly, in Sec. 3.3, we present the human evaluation process to assess the correlation between the I²EBench score and the human score. *A detailed explanation can be found in the supplementary materials.*

3.1 Evaluation Dimension

In our evaluation of the IIE model’s editing quality, we have categorized it into 16 dimensions, each assessing different aspects of editing in a top-down manner. An overview of I²EBench is presented in Fig. 1. High-level Editing Evaluation primarily focuses on assessing the model’s ability to accurately understand instructions and make precise edits to local areas of the input image. This evaluation consists of 8 dimensions. Low-level Editing Evaluation, on the other hand, primarily examines global editing and detailed image processing. It also comprises 8 evaluation dimensions. Unlike previous approaches [Fu et al. \[2024\]](#), [Zhang et al. \[2023a\]](#), [Geng et al. \[2023\]](#) that relied on a single metric, such as CLIP score [Radford et al. \[2021\]](#), to evaluate editing quality for all editing types, we have developed specialized evaluation methods for each of the 16 dimensions. This approach is necessary due to the distinct goals of high-level and low-level editing.

3.1.1 High-level Editing

Evaluating editing quality in high-level dimensions poses a challenge due to the diverse goals involved, making it impractical to rely on a single metric. The advancement of Multimodal Large Language Models (MLLM) [Gao et al. \[2024\]](#), [Chu et al. \[2024\]](#), [Zhu et al. \[2024\]](#), [Dong et al. \[2024a,b\]](#), [Wei et al. \[2024\]](#), [Young et al. \[2024\]](#), such as GPT-4V [Achiam et al. \[2023\]](#), Gemini Pro [Reid et al. \[2024\]](#), and QWen-VL-Plus [Bai et al. \[2023\]](#), has significantly enhanced automated understanding of images. Therefore, to ensure precise evaluation of the editing quality of IIE models in high-level dimensions, we leverage the exceptional capabilities of the widely recognized GPT-4V model to make judgments for most high-level evaluation dimensions.

Counting. The Counting dimension pertains to instructions related to the number of objects, such as "add two apples to the image." To assess this dimension, we query GPT-4V about the number of target objects in the image and compare its response with the human-annotated answer.

Direction Perception. The Direction Perception dimension requires the IIE model to comprehend directions provided in instructions, and accurately make edits when presented with images. We evaluate this dimension by asking GPT-4V if the target object is in the expected position.

Object Removal. The Object Removal dimension focuses on removing the target object according to the given instruction. To evaluate this dimension, we inquire whether GPT-4V identifies the presence of the target object in the image.

Object Replacement. The Object Replacement dimension aims to replace the original object with the target object as instructed. To assess this dimension, we query GPT-4V about the presence of the target object in the image.

Background Replacement. The Background Replacement dimension involves replacing the original background with the target background as specified in the instruction. To evaluate this dimension, we ask GPT-4V if the background of the image matches the textual instruction.

Color Alteration. In the Color Alteration dimension, we modify the color of the target object using instructions. To evaluate this dimension, we inquire GPT-4V about the color of the target object in the edited image.

Style Alteration. The Style Alteration dimension focuses on changing the style of the image. To evaluate this dimension, we calculate the CLIP similarity [Radford et al. \[2021\]](#) between the edited image and "an image with ... style".

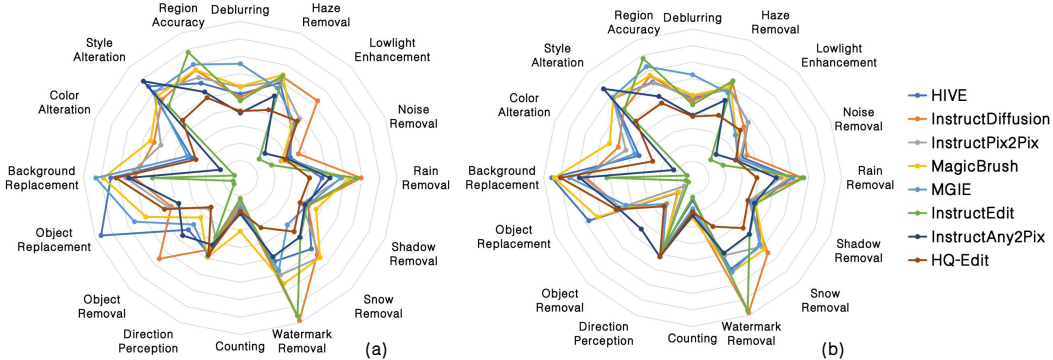


Figure 4: Comparison of radar charts for I²EBench scores in different dimensions using (a) original instructions and (b) diverse instructions.

instructions. Fig. 3 (a) and (b) present the word cloud visualizations of the original and diverse instructions, respectively. Additionally, we also annotate a category for each instruction, such as animal, object, scenery, plant, human, and global.

Evaluation Annotation. The evaluation process for I²EBench encompasses two distinct categories. The first category employs conventional metrics to assess various dimensions. For style alteration dimension, we utilize the CLIP score as a standard metric, which doesn’t need any additional evaluation annotations. In the second category, we utilize GPT-4V to evaluate the quality of editing. To facilitate this evaluation, we enlisted the expertise of human annotators to annotate questions specifically designed for GPT-4V, along with corresponding standard answers. For instance, let’s consider the counting dimension and the instruction "Add a cat to the shoe rack". In this particular case, the annotated question provided by the human annotators is "How many cats are there on the shoe rack?", and the corresponding annotated answer is "One".

3.3 Human Evaluation

The primary objective of the human evaluation is to ascertain the correlation between human perception and the I²EBench score. To achieve this, we present human evaluators with a textual instruction T , an input image V_I , and a set of edited images $\{V_1, V_2, \dots, V_M\}$ generated by M different IIE models. The evaluators are then tasked with ranking the results based on their judgment. More specifically, we sample N images for each evaluation dimension, leading to a comprehensive collection of $N \times 16 \times 2$ edited image comparisons. Within each comparison, evaluators are presented with M edited images to assess and rank in relation to one another. We assign a human score to each model based on its ranking among the M models. Specifically, the model ranked first among the M models receives a human score of M , while the model ranked last among the M models receives a human score of 1. Additionally, the model ranked k among the M models is assigned a human score of $M - k + 1$. To determine the human score for each dimension, we calculate the average of the human scores across all samples within that dimension. Thus, the human score for each model ranges from 1 to M .

4 Experiments

Dimension Evaluation. For each image and instruction, we utilize official codes from various models for image editing. We calculate the I²EBench scores following the methodology described in Sec.3.1. The I²EBench scores for original and diverse instructions are presented in Fig. 4, Tab.1, and Tab. 2, respectively. Our observations reveal that no single model achieves the best performance across all evaluation dimensions. Regarding low-level editing, InstructDiffusion Geng et al. [2023] demonstrates superior results. It attains the highest scores in 4 out of 7 low-level editing evaluation dimensions when using original instructions, and 3 out of 7 when using diverse instructions. For high-level editing, both MagicBrush Zhang et al. [2024a] and InstructAny2Pix Li et al. [2023e] perform impressively. MagicBrush achieves the highest scores in 3 evaluation dimensions using original instructions, while InstructAny2Pix achieves the highest scores in 3 dimensions using diverse

Table 1: I²EBench evaluation results per dimension using original instructions. *Exp Min* and *Exp Max* denote the minimum and maximum values of all samples for each evaluation dimension.

Low-level Editing								
Model	Deblurring	Haze Removal	Lowlight Enhancement	Noise Removal	Rain Removal	Shadow Removal	Snow Removal	Watermark Removal
HIVE Zhang et al. [2023a]	44.25	54.89	37.61	24.59	45.47	37.61	51.49	49.99
InstructDiffusion Geng et al. [2023]	42.48	58.45	56.61	28.60	67.20	37.43	55.65	85.49
InstructPix2Pix Brooks et al. [2023]	48.03	56.15	43.32	20.11	56.64	34.19	57.59	58.12
MagicBrush Zhang et al. [2024a]	48.38	59.46	37.71	20.59	60.60	41.91	57.81	63.33
MGIE Fu et al. [2024]	60.30	51.75	39.99	23.25	56.00	36.91	34.04	55.53
InstructEdit Wang et al. [2023b]	40.77	58.85	13.83	15.40	64.44	36.88	43.45	82.68
InstructAny2Pix Li et al. [2023e]	34.34	47.27	18.03	22.89	49.94	35.84	42.97	47.28
HQ-Edit Hui et al. [2024]	35.27	39.25	41.71	22.13	38.52	33.13	38.97	29.80
Exp Min	13.79	12.66	0.09	0.79	7.38	1.05	2.18	1.34
Exp Max	91.94	92.70	89.60	77.00	96.11	89.19	89.26	96.42
High-level Editing								
Model	Counting	Direction Perception	Object Removal	Object Replacement	Background Replacement	Color Alteration	Style Alteration	Region Accuracy
HIVE Zhang et al. [2023a]	18.57	47.14	42.14	86.43	74.29	30.00	25.32	58.15
InstructDiffusion Geng et al. [2023]	15.00	44.29	65.71	42.86	60.71	53.57	21.69	66.18
InstructPix2Pix Brooks et al. [2023]	13.57	37.14	25.00	44.29	65.71	49.29	23.76	61.63
MagicBrush Zhang et al. [2024a]	30.71	49.29	32.14	58.57	78.57	55.71	22.78	66.34
MGIE Fu et al. [2024]	17.14	48.57	37.86	65.71	82.86	32.86	23.68	69.60
InstructEdit Wang et al. [2023b]	11.76	41.73	5.04	4.41	50.36	3.62	19.83	77.08
InstructAny2Pix Li et al. [2023e]	20.59	41.73	46.76	38.24	64.03	12.32	26.76	52.75
HQ-Edit Hui et al. [2024]	19.26	47.79	23.74	47.06	71.22	27.54	15.96	49.21
Exp Min	0.00	0.00	0.00	0.00	0.00	0.00	12.96	6.41
Exp Max	100.00	100.00	100.00	100.00	100.00	100.00	33.84	98.70

Table 2: I²EBench evaluation results per dimension using diverse instructions.

Low-level Editing								
Model	Deblurring	Haze Removal	Lowlight Enhancement	Noise Removal	Rain Removal	Shadow Removal	Snow Removal	Watermark Removal
HIVE Zhang et al. [2023a]	44.41	54.09	42.78	25.51	58.59	36.69	51.92	57.88
InstructDiffusion Geng et al. [2023]	42.62	58.01	39.47	28.06	64.18	32.54	57.30	85.14
InstructPix2Pix Brooks et al. [2023]	45.24	53.52	42.88	24.49	51.86	32.79	52.67	48.91
MagicBrush Zhang et al. [2024a]	45.96	55.11	33.74	23.91	55.77	36.73	54.68	59.76
MGIE Fu et al. [2024]	57.33	51.61	32.96	23.49	58.27	34.07	51.02	59.64
InstructEdit Wang et al. [2023b]	40.66	58.89	13.92	15.81	65.08	36.66	43.34	83.68
InstructAny2Pix Li et al. [2023e]	34.77	47.00	18.09	22.18	48.92	36.04	43.13	47.58
HQ-Edit Hui et al. [2024]	34.11	37.95	36.76	22.38	37.60	32.17	38.45	30.83
Exp Min	6.32	3.67	0.60	0.03	7.22	1.46	3.78	2.58
Exp Max	88.17	92.69	90.34	79.29	97.03	86.27	82.24	96.39
High-level Editing								
Model	Counting	Direction Perception	Object Removal	Object Replacement	Background Replacement	Color Alteration	Style Alteration	Region Accuracy
HIVE Zhang et al. [2023a]	13.57	43.57	12.86	67.86	85.00	35.00	23.08	61.97
InstructDiffusion Geng et al. [2023]	21.43	47.86	22.14	47.14	64.29	48.57	19.96	65.92
InstructPix2Pix Brooks et al. [2023]	18.57	47.86	7.14	47.14	65.71	43.57	23.13	61.32
MagicBrush Zhang et al. [2024a]	24.29	45.71	12.14	62.14	83.57	54.29	23.08	66.21
MGIE Fu et al. [2024]	19.29	47.14	22.86	43.57	74.29	37.86	23.36	71.89
InstructEdit Wang et al. [2023b]	11.76	46.04	3.60	4.41	51.80	3.62	19.91	77.08
InstructAny2Pix Li et al. [2023e]	22.79	51.80	43.88	48.53	68.35	12.32	25.93	52.61
HQ-Edit Hui et al. [2024]	20.74	51.47	24.46	50.00	79.86	26.09	16.48	48.29
Exp Min	0.00	0.00	0.00	0.00	0.00	0.00	10.62	9.79
Exp Max	100.00	100.00	100.00	100.00	100.00	100.00	34.06	98.68

instructions. In the deblurring dimensions, MGIE Fu et al. [2024] stands out significantly. It surpasses the second-place model by 11.92 when using original instructions and by 11.37 when using diverse instructions.

Human Evaluation. We ranked different models based on their I²EBench scores and computed I²EBench rank scores using the methodology described in Sec. 3.3. Given that both I²EBench rank scores and human scores range from 1 to 8, a direct comparison can be made between them. Therefore, we conducted correlation analyses and visually presented the results in Fig. 5. Significant positive correlations were observed between the I²EBench rank score and the human score across all dimensions. These findings offer strong evidence supporting the alignment between our proposed benchmark and human perception.

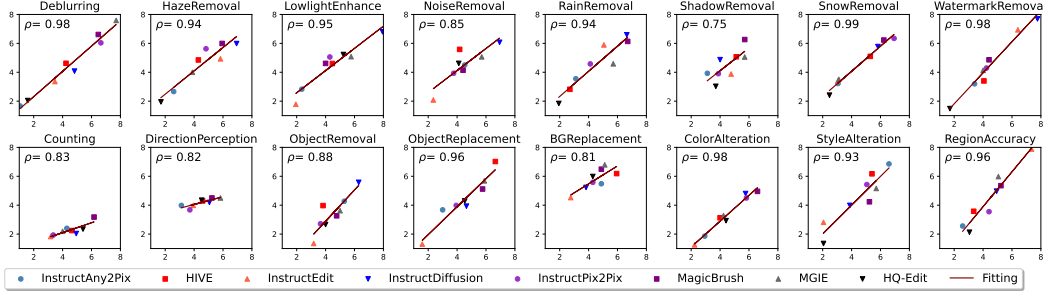


Figure 5: Alignment between I²EBench rank scores (Y-axis) and human scores (X-axis).

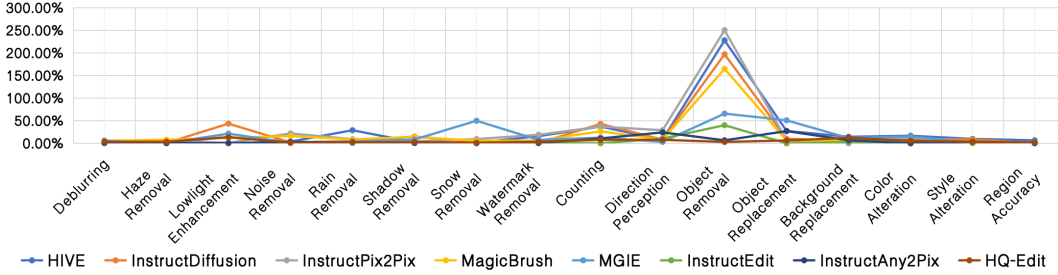


Figure 6: I²EBench change rate using original instructions and diverse instructions.

5 Insights

The editing ability across different dimensions is not robust: Our observations indicate that no single model excels in all evaluation dimensions. This implies that different IIE models have varying strengths in terms of their editing abilities across different dimensions. Thus, it is crucial to acknowledge this limitation and focus on developing an IIE model that demonstrates consistent and competent performance across all dimensions. *Future research efforts should prioritize the creation of a robust and versatile IIE model that can effectively handle a wide range of editing tasks across diverse dimensions.*

The editing ability of different instructions is not robust: To evaluate the robustness of editing models when provided with different instructions, we propose a metric called I²EBench change rate. This metric is defined as follows:

$$S^i = \frac{|S_o^i - S_d^i|}{\text{MIN}(S_o^i, S_d^i)}, \quad (1)$$

where S_o^i and S_d^i represent the I²EBench scores of the i -th evaluation dimension when using original and diverse instructions, respectively. The value of S^i indicates the I²EBench change rate for the i -th evaluation dimension. As illustrated in Fig. 6, when it comes to the object removal dimension, InstructPix2Pix Brooks et al. [2023], HIVE Zhang et al. [2023a], InstructionDiffusion Geng et al. [2023], and MagicBrush Zhang et al. [2024a] exhibit significant fluctuations in their performance using different instructions. On the other hand, the remaining models demonstrate relatively stable performance across different instructions. One notable distinction between these two categories of models is that the latter employs LLM Achiam et al. [2023], Touvron et al. [2023] or MLLM Liu et al. [2023b,a] to comprehend instructions, which enhances their resilience to variations in instructions. *Given the unpredictable and diverse nature of user editing instructions, it is crucial to develop an editing model that can effectively handle instructions with varying levels of complexity.*

The editing ability for different categories is not robust: As illustrated in Fig. 7, we have observed distinct variations in the performance of different categories. Notably, the "Scenery" and "Global" categories consistently demonstrate superior performance compared to the other categories across all the IIE models we evaluated. This discrepancy can be attributed to the inherent inclination of the "Scenery" and "Global" categories towards global editing, which diminishes the necessity for

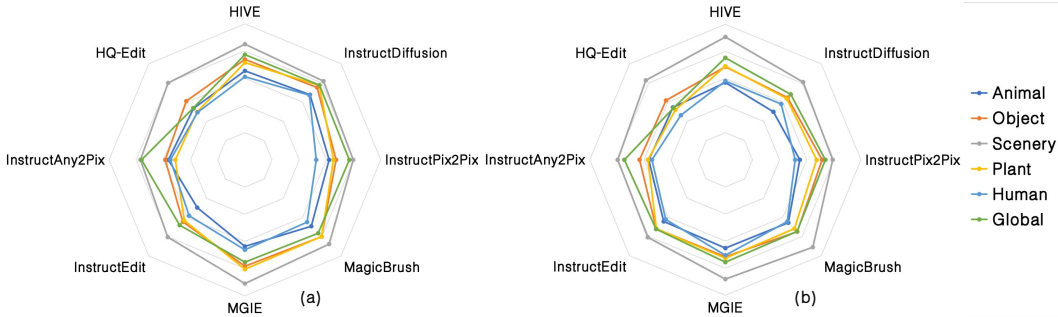


Figure 7: Comparison of radar charts for I²EBench scores in different categories using (a) original instructions and (b) diverse instructions. The scores of all dimensions are normalized and averaged.

precise target object localization. *Given these findings, it is crucial to prioritize the simultaneous consideration of various editing content in future research endeavors.*

6 Conclusions

In this paper, we present I²EBench, a comprehensive benchmark specifically designed for instruction-based image editing (IIE). Our benchmark includes a substantial dataset of over 2000+ images and more than 4000+ instructions, covering 16 distinct evaluation dimensions. To evaluate the effectiveness of I²EBench, we conduct experiments using 8 open-source IIE models. Additionally, we complement these experiments with meticulous human evaluations to establish the correlation between I²EBench scores and human perception. Based on the observations derived from I²EBench, we provide valuable insights and recommendations for advancing IIE models. We hope the proposed I²EBench to serve as an indispensable asset, playing a pivotal role in fostering the advancement of IIE models and assessing their efficacy.

References

- Josh Achiam, Steven Adler, Sandhini Agarwal, Lama Ahmad, Ilge Akkaya, Florencia Leoni Aleman, Diogo Almeida, Janko Alvenschmidt, Sam Altman, Shyamal Anadkat, et al. Gpt-4 technical report. *arXiv preprint arXiv:2303.08774*, 2023.
- Jean-Baptiste Alayrac, Jeff Donahue, Pauline Luc, Antoine Miech, Iain Barr, Yana Hasson, Karel Lenc, Arthur Mensch, Katherine Millican, Malcolm Reynolds, et al. Flamingo: a visual language model for few-shot learning. *Advances in neural information processing systems*, 35:23716–23736, 2022.
- Codruta O Ancuti, Cosmin Ancuti, Mateu Sbert, and Radu Timofte. Dense-haze: A benchmark for image dehazing with dense-haze and haze-free images. In *2019 IEEE international conference on image processing (ICIP)*, pages 1014–1018. IEEE, 2019.
- Jacob Austin, Daniel D Johnson, Jonathan Ho, Daniel Tarlow, and Rianne Van Den Berg. Structured denoising diffusion models in discrete state-spaces. *Advances in Neural Information Processing Systems*, 34:17981–17993, 2021.
- Omri Avrahami, Dani Lischinski, and Ohad Fried. Blended diffusion for text-driven editing of natural images. In *Proceedings of the IEEE/CVF Conference on Computer Vision and Pattern Recognition*, pages 18208–18218, 2022.
- Jinze Bai, Shuai Bai, Shusheng Yang, Shijie Wang, Sinan Tan, Peng Wang, Junyang Lin, Chang Zhou, and Jingren Zhou. Qwen-vl: A frontier large vision-language model with versatile abilities. *arXiv preprint arXiv:2308.12966*, 2023.
- Samyadeep Basu, Mehrdad Saberi, Shweta Bhardwaj, Atoosa Malemir Chegini, Daniela Massiceti, Maziar Sanjabi, Shell Xu Hu, and Soheil Feizi. Editval: Benchmarking diffusion based text-guided image editing methods. *arXiv preprint arXiv:2310.02426*, 2023.
- James Betker, Gabriel Goh, Li Jing, Tim Brooks, Jianfeng Wang, Linjie Li, Long Ouyang, Juntang Zhuang, Joyce Lee, Yufei Guo, et al. Improving image generation with better captions. *Computer Science. https://cdn.openai.com/papers/dall-e-3.pdf*, 2(3):8, 2023.

- Jeffrey P Bigam, Chandrika Jayant, Hanjie Ji, Greg Little, Andrew Miller, Robert C Miller, Robin Miller, Aubrey Tatarowicz, Brandyn White, Samuel White, et al. Vizwiz: nearly real-time answers to visual questions. In *Proceedings of the 23rd annual ACM symposium on User interface software and technology*, pages 333–342, 2010.
- Tim Brooks, Aleksander Holynski, and Alexei A Efros. Instructpix2pix: Learning to follow image editing instructions. In *Proceedings of the IEEE/CVF Conference on Computer Vision and Pattern Recognition*, pages 18392–18402, 2023.
- Tom Brown, Benjamin Mann, Nick Ryder, Melanie Subbiah, Jared D Kaplan, Prafulla Dhariwal, Arvind Neelakantan, Pranav Shyam, Girish Sastry, Amanda Askell, et al. Language models are few-shot learners. *Advances in neural information processing systems*, 33:1877–1901, 2020.
- Haoyu Chen, Jinjin Gu, Yihao Liu, Salma Abdel Magid, Chao Dong, Qiong Wang, Hanspeter Pfister, and Lei Zhu. Masked image training for generalizable deep image denoising. In *Proceedings of the IEEE/CVF Conference on Computer Vision and Pattern Recognition*, pages 1692–1703, 2023a.
- Wei-Ting Chen, Hao-Yu Fang, Cheng-Lin Hsieh, Cheng-Che Tsai, I Chen, Jian-Jiun Ding, Sy-Yen Kuo, et al. All snow removed: Single image desnowing algorithm using hierarchical dual-tree complex wavelet representation and contradict channel loss. In *Proceedings of the IEEE/CVF International Conference on Computer Vision*, pages 4196–4205, 2021.
- Xiang Chen, Hao Li, Mingqiang Li, and Jinshan Pan. Learning a sparse transformer network for effective image deraining. In *Proceedings of the IEEE/CVF Conference on Computer Vision and Pattern Recognition*, pages 5896–5905, 2023b.
- Yang Chen, Yu-Kun Lai, and Yong-Jin Liu. CartoonGAN: Generative adversarial networks for photo cartoonization. In *Proceedings of the IEEE conference on computer vision and pattern recognition*, pages 9465–9474, 2018.
- Xiangxiang Chu, Limeng Qiao, Xinyu Zhang, Shuang Xu, Fei Wei, Yang Yang, Xiaofei Sun, Yiming Hu, Xinyang Lin, Bo Zhang, et al. MobileVLM v2: Faster and stronger baseline for vision language model. *arXiv preprint arXiv:2402.03766*, 2024.
- Wenliang Dai, Junnan Li, Dongxu Li, Anthony Meng Huat Tiong, Junqi Zhao, Weisheng Wang, Boyang Li, Pascale N Fung, and Steven Hoi. InstructBLIP: Towards general-purpose vision-language models with instruction tuning. *Advances in Neural Information Processing Systems*, 36, 2024.
- Tim Dockhorn, Arash Vahdat, and Karsten Kreis. Genie: Higher-order denoising diffusion solvers. *Advances in Neural Information Processing Systems*, 35:30150–30166, 2022.
- Wenkai Dong, Song Xue, Xiaoyue Duan, and Shumin Han. Prompt tuning inversion for text-driven image editing using diffusion models. In *Proceedings of the IEEE/CVF International Conference on Computer Vision*, pages 7430–7440, 2023.
- Xiaoyi Dong, Pan Zhang, Yuhang Zang, Yuhang Cao, Bin Wang, Linke Ouyang, Xilin Wei, Songyang Zhang, Haodong Duan, Maosong Cao, et al. InternLM-xcomposer2: Mastering free-form text-image composition and comprehension in vision-language large model. *arXiv preprint arXiv:2401.16420*, 2024a.
- Xiaoyi Dong, Pan Zhang, Yuhang Zang, Yuhang Cao, Bin Wang, Linke Ouyang, Songyang Zhang, Haodong Duan, Wenwei Zhang, Yining Li, et al. InternLM-xcomposer2-4khd: A pioneering large vision-language model handling resolutions from 336 pixels to 4k hd. *arXiv preprint arXiv:2404.06512*, 2024b.
- Tsu-Jui Fu, Wenze Hu, Xianzhi Du, William Yang Wang, Yinfei Yang, and Zhe Gan. Guiding instruction-based image editing via multimodal large language models. *International Conference on Learning Representations*, 2024.
- Peng Gao, Renrui Zhang, Chris Liu, Longtian Qiu, Siyuan Huang, Weifeng Lin, Shitian Zhao, Shijie Geng, Ziyi Lin, Peng Jin, et al. Sphinx-x: Scaling data and parameters for a family of multi-modal large language models. *arXiv preprint arXiv:2402.05935*, 2024.
- Zigang Geng, Binxin Yang, Tiankai Hang, Chen Li, Shuyang Gu, Ting Zhang, Jianmin Bao, Zheng Zhang, Han Hu, Dong Chen, et al. InstructDiffusion: A generalist modeling interface for vision tasks. *arXiv preprint arXiv:2309.03895*, 2023.
- Ian Goodfellow, Jean Pouget-Abadie, Mehdi Mirza, Bing Xu, David Warde-Farley, Sherjil Ozair, Aaron Courville, and Yoshua Bengio. Generative adversarial nets. *Advances in neural information processing systems*, 27, 2014.

- Ian Goodfellow, Jean Pouget-Abadie, Mehdi Mirza, Bing Xu, David Warde-Farley, Sherjil Ozair, Aaron Courville, and Yoshua Bengio. Generative adversarial networks. *Communications of the ACM*, 63(11): 139–144, 2020.
- Lanqing Guo, Chong Wang, Wenhan Yang, Siyu Huang, Yufei Wang, Hanspeter Pfister, and Bihan Wen. Shadowdiffusion: When degradation prior meets diffusion model for shadow removal. In *Proceedings of the IEEE/CVF Conference on Computer Vision and Pattern Recognition*, pages 14049–14058, 2023a.
- Yun Guo, Xueyao Xiao, Yi Chang, Shumin Deng, and Luxin Yan. From sky to the ground: A large-scale benchmark and simple baseline towards real rain removal. In *Proceedings of the IEEE/CVF International Conference on Computer Vision*, pages 12097–12107, 2023b.
- Amir Hertz, Ron Mokady, Jay Tenenbaum, Kfir Aberman, Yael Pritch, and Daniel Cohen-Or. Prompt-to-prompt image editing with cross attention control. *arXiv preprint arXiv:2208.01626*, 2022.
- Jonathan Ho, Ajay Jain, and Pieter Abbeel. Denoising diffusion probabilistic models. *Advances in neural information processing systems*, 33:6840–6851, 2020.
- Anwen Hu, Haiyang Xu, Jiabo Ye, Ming Yan, Liang Zhang, Bo Zhang, Chen Li, Ji Zhang, Qin Jin, Fei Huang, et al. mplug-docowl 1.5: Unified structure learning for ocr-free document understanding. *arXiv preprint arXiv:2403.12895*, 2024.
- Yi Huang, Jiancheng Huang, Yifan Liu, Mingfu Yan, Jiayi Lv, Jianzhuang Liu, Wei Xiong, He Zhang, Shifeng Chen, and Liangliang Cao. Diffusion model-based image editing: A survey. *arXiv preprint arXiv:2402.17525*, 2024a.
- Yuzhou Huang, Liangbin Xie, Xintao Wang, Ziyang Yuan, Xiaodong Cun, Yixiao Ge, Jiantao Zhou, Chao Dong, Rui Huang, Ruimao Zhang, et al. Smartedit: Exploring complex instruction-based image editing with multimodal large language models. *Proceedings of the IEEE/CVF Conference on Computer Vision and Pattern Recognition*, 2024b.
- Drew A Hudson and Christopher D Manning. Gqa: A new dataset for real-world visual reasoning and compositional question answering. In *Proceedings of the IEEE/CVF conference on computer vision and pattern recognition*, pages 6700–6709, 2019.
- Mude Hui, Siwei Yang, Bingchen Zhao, Yichun Shi, Heng Wang, Peng Wang, Yuyin Zhou, and Cihang Xie. Hq-edit: A high-quality dataset for instruction-based image editing. *arXiv preprint arXiv:2404.09990*, 2024.
- Tero Karras, Samuli Laine, and Timo Aila. A style-based generator architecture for generative adversarial networks. In *Proceedings of the IEEE/CVF conference on computer vision and pattern recognition*, pages 4401–4410, 2019.
- Tero Karras, Miika Aittala, Janne Hellsten, Samuli Laine, Jaakko Lehtinen, and Timo Aila. Training generative adversarial networks with limited data. *Advances in neural information processing systems*, 33:12104–12114, 2020a.
- Tero Karras, Samuli Laine, Miika Aittala, Janne Hellsten, Jaakko Lehtinen, and Timo Aila. Analyzing and improving the image quality of stylegan. In *Proceedings of the IEEE/CVF conference on computer vision and pattern recognition*, pages 8110–8119, 2020b.
- Bahjat Kawar, Michael Elad, Stefano Ermon, and Jiaming Song. Denoising diffusion restoration models. *Advances in Neural Information Processing Systems*, 35:23593–23606, 2022.
- Bahjat Kawar, Shiran Zada, Oran Lang, Omer Tov, Huiwen Chang, Tali Dekel, Inbar Mosseri, and Michal Irani. Imagic: Text-based real image editing with diffusion models. In *Proceedings of the IEEE/CVF Conference on Computer Vision and Pattern Recognition*, pages 6007–6017, 2023.
- Xiangtao Kong, Xina Liu, Jinjin Gu, Yu Qiao, and Chao Dong. Reflash dropout in image super-resolution. In *Proceedings of the IEEE/CVF Conference on Computer Vision and Pattern Recognition*, pages 6002–6012, 2022.
- Jari Korhonen and Junyong You. Peak signal-to-noise ratio revisited: Is simple beautiful? In *2012 Fourth International Workshop on Quality of Multimedia Experience*, pages 37–38. IEEE, 2012.
- Vladimir Kulikov, Shahar Yadin, Matan Kleiner, and Tomer Michaeli. Sinddm: A single image denoising diffusion model. In *International Conference on Machine Learning (ICML)*, pages 17920–17930. PMLR, 2023.

- Bohao Li, Rui Wang, Guangzhi Wang, Yuying Ge, Yixiao Ge, and Ying Shan. Seed-bench: Benchmarking multimodal llms with generative comprehension. *arXiv preprint arXiv:2307.16125*, 2023a.
- Junnan Li, Dongxu Li, Caiming Xiong, and Steven Hoi. Blip: Bootstrapping language-image pre-training for unified vision-language understanding and generation. In *International conference on machine learning (ICML)*, 2022.
- Junnan Li, Dongxu Li, Silvio Savarese, and Steven Hoi. Blip-2: Bootstrapping language-image pre-training with frozen image encoders and large language models. In *International conference on machine learning*, pages 19730–19742. PMLR, 2023b.
- Junnan Li, Dongxu Li, Silvio Savarese, and Steven Hoi. BLIP-2: bootstrapping language-image pre-training with frozen image encoders and large language models. In *International conference on machine learning (ICML)*, 2023c.
- Kunchang Li, Yali Wang, Yinan He, Yizhuo Li, Yi Wang, Yi Liu, Zun Wang, Jilan Xu, Guo Chen, Ping Luo, et al. Mvbench: A comprehensive multi-modal video understanding benchmark. *arXiv preprint arXiv:2311.17005*, 2023d.
- Shufan Li, Harkanwar Singh, and Aditya Grover. Instructany2pix: Flexible visual editing via multimodal instruction following. *arXiv preprint arXiv:2312.06738*, 2023e.
- Yifan Li, Yifan Du, Kun Zhou, Jinpeng Wang, Wayne Xin Zhao, and Ji-Rong Wen. Evaluating object hallucination in large vision-language models. *arXiv preprint arXiv:2305.10355*, 2023f.
- Tsung-Yi Lin, Michael Maire, Serge Belongie, James Hays, Pietro Perona, Deva Ramanan, Piotr Dollár, and C Lawrence Zitnick. Microsoft coco: Common objects in context. In *Computer Vision—ECCV 2014: 13th European Conference, Zurich, Switzerland, September 6-12, 2014, Proceedings, Part V 13*, pages 740–755. Springer, 2014.
- Haotian Liu, Chunyuan Li, Yuheng Li, and Yong Jae Lee. Improved baselines with visual instruction tuning, 2023a.
- Haotian Liu, Chunyuan Li, Qingyang Wu, and Yong Jae Lee. Visual instruction tuning, 2023b.
- Haotian Liu, Chunyuan Li, Yuheng Li, Bo Li, Yuanhan Zhang, Sheng Shen, and Yong Jae Lee. Llava-next: Improved reasoning, ocr, and world knowledge, January 2024. URL <https://llava-vl.github.io/blog/2024-01-30-llava-next/>.
- Yang Liu, Zhen Zhu, and Xiang Bai. Wdnet: Watermark-decomposition network for visible watermark removal. In *2021 IEEE/CVF Winter Conference on Applications of Computer Vision (WACV)*. IEEE, 2021a.
- Ye Liu, Lei Zhu, Shunda Pei, Huazhu Fu, Jing Qin, Qing Zhang, Liang Wan, and Wei Feng. From synthetic to real: Image dehazing collaborating with unlabeled real data. In *Proceedings of the 29th ACM international conference on multimedia*, pages 50–58, 2021b.
- Pan Lu, Swaroop Mishra, Tanglin Xia, Liang Qiu, Kai-Wei Chang, Song-Chun Zhu, Oyvind Tafjord, Peter Clark, and Ashwin Kalyan. Learn to explain: Multimodal reasoning via thought chains for science question answering. *Advances in Neural Information Processing Systems*, 35:2507–2521, 2022.
- Xudong Mao, Qing Li, Haoran Xie, Raymond YK Lau, Zhen Wang, and Stephen Paul Smolley. Least squares generative adversarial networks. In *Proceedings of the IEEE international conference on computer vision*, pages 2794–2802, 2017.
- Kenneth Marino, Mohammad Rastegari, Ali Farhadi, and Roozbeh Mottaghi. Ok-vqa: A visual question answering benchmark requiring external knowledge. In *Proceedings of the IEEE/cvf conference on computer vision and pattern recognition*, pages 3195–3204, 2019.
- D. Martin, C. Fowlkes, D. Tal, and J. Malik. A database of human segmented natural images and its application to evaluating segmentation algorithms and measuring ecological statistics. In *Proc. 8th Int’l Conf. Computer Vision*, volume 2, pages 416–423, July 2001.
- Seungjun Nah, Tae Hyun Kim, and Kyoung Mu Lee. Deep multi-scale convolutional neural network for dynamic scene deblurring. In *The IEEE Conference on Computer Vision and Pattern Recognition (CVPR)*, July 2017.
- Alexander Quinn Nichol and Prafulla Dhariwal. Improved denoising diffusion probabilistic models. In *International conference on machine learning*, pages 8162–8171. PMLR, 2021.

- Liangqiong Qu, Jiandong Tian, Shengfeng He, Yandong Tang, and Rynson WH Lau. Deshadownet: A multi-context embedding deep network for shadow removal. In *Proceedings of the IEEE conference on computer vision and pattern recognition*, pages 4067–4075, 2017.
- Alec Radford, Jong Wook Kim, Chris Hallacy, Aditya Ramesh, Gabriel Goh, Sandhini Agarwal, Girish Sastry, Amanda Askell, Pamela Mishkin, Jack Clark, et al. Learning transferable visual models from natural language supervision. In *International conference on machine learning (ICML)*, pages 8748–8763. PMLR, 2021.
- Aditya Ramesh, Mikhail Pavlov, Gabriel Goh, Scott Gray, Chelsea Voss, Alec Radford, Mark Chen, and Ilya Sutskever. Zero-shot text-to-image generation. In *International conference on machine learning*, pages 8821–8831. Pmlr, 2021.
- Aditya Ramesh, Prafulla Dhariwal, Alex Nichol, Casey Chu, and Mark Chen. Hierarchical text-conditional image generation with clip latents. *arXiv preprint arXiv:2204.06125*, 1(2):3, 2022.
- Machel Reid, Nikolay Savinov, Denis Teplyashin, Dmitry Lepikhin, Timothy Lillicrap, Jean-baptiste Alayrac, Radu Soricut, Angeliki Lazaridou, Orhan Firat, Julian Schrittwieser, et al. Gemini 1.5: Unlocking multimodal understanding across millions of tokens of context. *arXiv preprint arXiv:2403.05530*, 2024.
- Robin Rombach, Andreas Blattmann, Dominik Lorenz, Patrick Esser, and Björn Ommer. High-resolution image synthesis with latent diffusion models. In *Proceedings of the IEEE/CVF conference on computer vision and pattern recognition*, pages 10684–10695, 2022.
- Chitwan Saharia, William Chan, Saurabh Saxena, Lala Li, Jay Whang, Emily L Denton, Kamyar Ghasemipour, Raphael Gontijo Lopes, Burcu Karagol Ayan, Tim Salimans, et al. Photorealistic text-to-image diffusion models with deep language understanding. *Advances in neural information processing systems*, 35:36479–36494, 2022.
- Yash Sanghvi, Zhiyuan Mao, and Stanley H Chan. Structured kernel estimation for photon-limited deconvolution. In *Proceedings of the IEEE/CVF Conference on Computer Vision and Pattern Recognition*, pages 9863–9872, 2023.
- Eric Saund, David Fleet, Daniel Lerner, and James Mahoney. Perceptually-supported image editing of text and graphics. In *Proceedings of the 16th annual ACM symposium on User interface software and technology*, pages 183–192, 2003.
- Ziyi Shen, Wenguan Wang, Xiankai Lu, Jianbing Shen, Haibin Ling, Tingfa Xu, and Ling Shao. Human-aware motion deblurring. In *Proceedings of the IEEE/CVF International Conference on Computer Vision*, pages 5572–5581, 2019.
- Shelly Sheynin, Adam Polyak, Uriel Singer, Yuval Kirstain, Amit Zohar, Oron Ashual, Devi Parikh, and Yaniv Taigman. Emu edit: Precise image editing via recognition and generation tasks. *arXiv preprint arXiv:2311.10089*, 2023.
- Jascha Sohl-Dickstein, Eric Weiss, Niru Maheswaranathan, and Surya Ganguli. Deep unsupervised learning using nonequilibrium thermodynamics. In *International conference on machine learning (ICML)*, pages 2256–2265. PMLR, 2015.
- Jiaming Song, Chenlin Meng, and Stefano Ermon. Denoising diffusion implicit models. *arXiv preprint arXiv:2010.02502*, 2020.
- Hugo Touvron, Thibaut Lavril, Gautier Izacard, Xavier Martinet, Marie-Anne Lachaux, Timothée Lacroix, Baptiste Rozière, Naman Goyal, Eric Hambro, Faisal Azhar, et al. Llama: Open and efficient foundation language models. *arXiv preprint arXiv:2302.13971*, 2023.
- Dani Valevski, Matan Kalman, Eyal Molad, Eyal Segalis, Yossi Matias, and Yaniv Leviathan. Unitune: Text-driven image editing by fine tuning a diffusion model on a single image. *ACM Transactions on Graphics (TOG)*, 42(4):1–10, 2023.
- Hang Wang, Xuanhong Chen, Bingbing Ni, Yutian Liu, and Jinfan Liu. Omni aggregation networks for lightweight image super-resolution. In *Proceedings of the IEEE/CVF Conference on Computer Vision and Pattern Recognition*, pages 22378–22387, 2023a.
- Qian Wang, Biao Zhang, Michael Birsak, and Peter Wonka. Instructedit: Improving automatic masks for diffusion-based image editing with user instructions. *arXiv preprint arXiv:2305.18047*, 2023b.
- Su Wang, Chitwan Saharia, Ceslee Montgomery, Jordi Pont-Tuset, Shai Noy, Stefano Pellegrini, Yasumasa Onoe, Sarah Laszlo, David J Fleet, Radu Soricut, et al. Imagen editor and editbench: Advancing and evaluating text-guided image inpainting. In *Proceedings of the IEEE/CVF conference on computer vision and pattern recognition*, pages 18359–18369, 2023c.

- Zhou Wang, Alan C Bovik, Hamid R Sheikh, and Eero P Simoncelli. Image quality assessment: from error visibility to structural similarity. *IEEE transactions on image processing*, 13(4):600–612, 2004.
- Chen Wei, Wenjing Wang, Wenhan Yang, and Jiaying Liu. Deep retinex decomposition for low-light enhancement. *arXiv preprint arXiv:1808.04560*, 2018.
- Haoran Wei, Lingyu Kong, Jinyue Chen, Liang Zhao, Zheng Ge, En Yu, Jianjian Sun, Chunrui Han, and Xiangyu Zhang. Small language model meets with reinforced vision vocabulary. *arXiv preprint arXiv:2401.12503*, 2024.
- Max Welling and Yee W Teh. Bayesian learning via stochastic gradient langevin dynamics. In *Proceedings of the 28th international conference on machine learning (ICML)*, pages 681–688, 2011.
- Chenfei Wu, Shengming Yin, Weizhen Qi, Xiaodong Wang, Zecheng Tang, and Nan Duan. Visual chatgpt: Talking, drawing and editing with visual foundation models. *arXiv preprint arXiv:2303.04671*, 2023a.
- Haoning Wu, Zicheng Zhang, Erli Zhang, Chaofeng Chen, Liang Liao, Annan Wang, Chunyi Li, Wenxiu Sun, Qiong Yan, Guangtao Zhai, et al. Q-bench: A benchmark for general-purpose foundation models on low-level vision. *arXiv preprint arXiv:2309.14181*, 2023b.
- Rui-Qi Wu, Zheng-Peng Duan, Chun-Le Guo, Zhi Chai, and Chongyi Li. Ridep: Revitalizing real image dehazing via high-quality codebook priors. In *Proceedings of the IEEE/CVF Conference on Computer Vision and Pattern Recognition*, pages 22282–22291, 2023c.
- Haiyang Xu, Qinghao Ye, Ming Yan, Yaya Shi, Jiabo Ye, Yuanhong Xu, Chenliang Li, Bin Bi, Qi Qian, Wei Wang, Guohai Xu, Ji Zhang, Songfang Huang, Fei Huang, and Jingren Zhou. mplug-2: A modularized multi-modal foundation model across text, image and video. In *International conference on machine learning (ICML)*, 2023.
- Sihan Xu, Ziqiao Ma, Yidong Huang, Honglak Lee, and Joyce Chai. Cyclenet: Rethinking cycle consistency in text-guided diffusion for image manipulation. *Advances in Neural Information Processing Systems*, 36, 2024.
- Qinghao Ye, Haiyang Xu, Guohai Xu, Jiabo Ye, Ming Yan, Yiyang Zhou, Junyang Wang, Anwen Hu, Pengcheng Shi, Yaya Shi, et al. mplug-owl: Modularization empowers large language models with multimodality. *arXiv preprint arXiv:2304.14178*, 2023.
- Jinsung Yoon, Daniel Jarrett, and Mihaela Van der Schaar. Time-series generative adversarial networks. *Advances in neural information processing systems*, 32, 2019.
- Alex Young, Bei Chen, Chao Li, Chengen Huang, Ge Zhang, Guanwei Zhang, Heng Li, Jiangcheng Zhu, Jianqun Chen, Jing Chang, et al. Yi: Open foundation models by 01. ai. *arXiv preprint arXiv:2403.04652*, 2024.
- Weihao Yu, Zhengyuan Yang, Linjie Li, Jianfeng Wang, Kevin Lin, Zicheng Liu, Xinchao Wang, and Lijuan Wang. Mm-vet: Evaluating large multimodal models for integrated capabilities. *arXiv preprint arXiv:2308.02490*, 2023.
- Han Zhang, Ian Goodfellow, Dimitris Metaxas, and Augustus Odena. Self-attention generative adversarial networks. In *International conference on machine learning*, pages 7354–7363. PMLR, 2019.
- Kai Zhang, Lingbo Mo, Wenhui Chen, Huan Sun, and Yu Su. Magicbrush: A manually annotated dataset for instruction-guided image editing. *Advances in Neural Information Processing Systems*, 36, 2024a.
- Richard Zhang, Phillip Isola, Alexei A Efros, Eli Shechtman, and Oliver Wang. The unreasonable effectiveness of deep features as a perceptual metric. In *Proceedings of the IEEE conference on computer vision and pattern recognition*, pages 586–595, 2018.
- Shu Zhang, Xinyi Yang, Yihao Feng, Can Qin, Chia-Chih Chen, Ning Yu, Zeyuan Chen, Huan Wang, Silvio Savarese, Stefano Ermon, et al. Hive: Harnessing human feedback for instructional visual editing. *arXiv preprint arXiv:2303.09618*, 2023a.
- Zhixing Zhang, Ligong Han, Arnab Ghosh, Dimitris N Metaxas, and Jian Ren. Sine: Single image editing with text-to-image diffusion models. In *Proceedings of the IEEE/CVF Conference on Computer Vision and Pattern Recognition*, pages 6027–6037, 2023b.
- Zhongping Zhang, Jian Zheng, Zhiyuan Fang, and Bryan A Plummer. Text-to-image editing by image information removal. In *Proceedings of the IEEE/CVF Winter Conference on Applications of Computer Vision*, pages 5232–5241, 2024b.
- Dongsheng Zhu, Xunzhu Tang, Weidong Han, Jinghui Lu, Yukun Zhao, Guoliang Xing, Junfeng Wang, and Dawei Yin. Vislinginstruct: Elevating zero-shot learning in multi-modal language models with autonomous instruction optimization. *arXiv preprint arXiv:2402.07398*, 2024.



(a) Add **a** tie to the man (easy)



(b) Add **three** birds to the skateboard (medium)



(c) Add **five** dogs to the image (hard)

Figure 8: **Visualization of Counting edit.** The images above show an original image (the first one of each row) and the editing result (the other five images of each row) with different editing models. As we can see in (a), most editing models are equipped with the capability of understanding a number like "one" or "a", but the task becomes more and more difficult with the increasing of the number. In (b), with the editing instruction *add three birds to the skateboard*, some models fail to edit the image correctly, and when the number reaches **five** in (c), all of the editing models can barely follow the instruction with such a large number.

A Appendix

A.1 More Details on Evaluation Dimension.

Counting. When using diffusion models to add some objects to the images, it is important for models to understand the numbers of the objects we want to add according to editing instructions. Thus, we provide the instructions like, *add a tie to the man*, *add three birds to the skateboard*, *add five dogs to the image*. As shown in Figure 8, editing instruction with a larger number means a much more difficult task, so we propose the editing model which can handle the number well should be better when evaluating the performance. To evaluate if the editing model successfully adds the specific number of objects to the image, we use GPT4V (with gpt-4-vision-preview checkpoint) to get the number of objects from the edited images, by designing the prompts, *i.e.*, *"How many ties are on the image?"*, *"How many birds are in the image?"*, *"How many dogs are in the image?"*. To restrain the useless and irrelevant context of the raw outputs of GPT4V, we also design a filter process with ChatGPT (with gpt-4-turbo checkpoint). For example, in Figure 8 (a), the GPT4V output is *"There is one tie visible in the image."*, and the prompt for ChatGPT final judge is shown below.

Question : *"How many ties are on the image?"*

Correct Answer : *"One"*

Machine Response : *"There is one tie visible in the image."*

Is the machine's answer correct? Answer yes or no.



(a) Add a man to the **left** of the road sign



(b) Add a knife to the **left** of the pineapple

Figure 9: **Visualization of Direction Perception edit.** The images above show an original image (the first one of each row) and the editing result (the other four images of each row) with different editing models. When using "Add a man to the **left** of the road sign" to edit the sample in the first row, almost all the models can add the man correctly, but in the sample of the second row, with the editing instruction "Add a knife to the **left** of the pineapple", the results show that the models are lack of the capability of distinguishing the direction in the instruction successfully. The last editing result perceives the direction though, but fail to add the correct object.

The "Question" is the prompt for GPT4V to perceive the number of objects in the edited image. The "Correct Answer" is the ground truth according to our editing prompt in the dataset. For example, if the editing prompt is "Add a tie to the man", the corresponding "Correct Answer" is "One". The "Machine Response" is the output of GPT4V using "Question" as the prompt for the edited image. And "Is the machine's answer correct? Answer yes or no." is the static prompt for ChatGPT final judgment. By this filtering process, the outputs of the ChatGPT are much more stable than using the regular matching method between GPT4V and Correct Answer directly, and almost all the outputs are "yes" or "no", instead of the long sentences with irrelevant information. With the help of the LVLMS, the scores of the models are calculated as:

$$\begin{aligned}
 X'_i &= Model(X_i) \\
 Machine\ Response_i &= GPT4V(Question_i, X'_i) \\
 Final\ Judgement_i &= ChatGPT(Question_i, Correct\ Answer_i, Machine\ Response_i) \\
 B_i &= \begin{cases} 1 & \text{"yes" in Final Judgement}_i \\ 0 & \text{else} \end{cases} \\
 S_{counting} &= \frac{1}{N_{counting}} \sum_{i=1}^{N_{counting}} B_i
 \end{aligned}$$

The X and X' represent the original image and edited image respectively, and the $Model$ is the editing model, $N_{counting}$ means the total number of samples in this Counting dataset, and $S_{counting}$ is the final score for the Counting dimension.

Direction Perception. To evaluate whether the editing model is equipped with the ability of direction perception, as shown in Figure 9, we design a strategy with LVLMS which is similar to the Counting evaluation. We first create the instructions and then edit the original image with the instructions. We still use GPT4V as LVLMS to ask the edited image if the object is added to the correct direction(as

a position sample) or another direction(as a negative sample). To make the results more stable, the ChatGPT is also used as a filter and do the final judgment.

More specifically, the *Question*, *Correct Answer*, *Machine Response* is designed for ChatGPT to get the final judgment like this:

Question : "Is the knife on the left of the pineapple? Answer Yes or No."

Correct Answer : "Yes"

Machine Response : "No"

Is the machine's answer correct? Answer yes or no.

With the output of the ChatGPT for the direction perception task, we summarize the process in the steps below:

$$\begin{aligned}
 X'_i &= Model(X_i) \\
 Machine\ Response_i &= GPT4V(Question_i, X'_i) \\
 Final\ Judgement_i &= ChatGPT(Question_i, Correct\ Answer_i, Machine\ Response_i) \\
 B_i &= \begin{cases} 1 & \text{"yes" in Final Judgement}_i \\ 0 & \text{else} \end{cases} \\
 S_{DirectionPerception} &= \frac{1}{N_{DirectionPerception}} \sum_{i=1}^{N_{DirectionPerception}} B_i
 \end{aligned}$$

Object Removal. As shown in Figure 10, this is also a significant dimension for an editing model. We use GPT4V as the LVM and ChatGPT for final judgment, and the object to be removed in editing instruction is designed including *animal*, *human*, *scenery*, *plant*, *etc.* After editing the original image, the GPT4V is used to ask if the object is in the edited image, then get the final judgment with ChatGPT. More specifically, the ChatGPT for object removal is designed like this:

Question : "Is there a boy in the image? Answer Yes or No."

Correct Answer : "No"

Machine Response : "Yes"

Is the machine's answer correct? Answer yes or no.

With the output of the ChatGPT for the object removal task, we summarize the process in the steps below:

$$\begin{aligned}
 X'_i &= Model(X_i) \\
 Machine\ Response_i &= GPT4V(Question_i, X'_i) \\
 Final\ Judgement_i &= ChatGPT(Question_i, Correct\ Answer_i, Machine\ Response_i) \\
 B_i &= \begin{cases} 1 & \text{"yes" in Final Judgement}_i \\ 0 & \text{else} \end{cases} \\
 S_{ObjectRemoval} &= \frac{1}{N_{ObjectRemoval}} \sum_{i=1}^{N_{ObjectRemoval}} B_i
 \end{aligned}$$

Object Replacement. As shown in Figure 11, this is a common dimension and is evaluated widely for an editing model. We still use GPT4V as the LVM and ChatGPT for final judgment, and the object to be replaced in editing instruction is designed including *animal*, *human*, *scenery*, *plant*, *etc.* After editing the original image, the GPT4V is used to ask if the object is replaced in the edited image, then get the final judgment with ChatGPT. The ChatGPT for object replacement is designed



(a) Remove the boys from the image



(b) Remove the mountains from the image



(c) Remove the setting sun from the image

Figure 10: **Visualization of Object Removal edit.** The images above show an original image (the first one of each row) and the editing result (the other four images of each row) with different editing models. In (a), the third result fails but the boys in most of the results are successfully removed. In (b), models are required to remove the mountains, which is a difficult task since the giant mountains are usually not easy to recognize. Some of the models fail but others remove the mountains and replace them with trees or sky. In (c), when trying to remove the setting sun from the image, almost none of the models can deal with the task, and the result in the third image removes the person incorrectly. These results indicate that most models are not equipped with the excellent ability of object removal.



(a) Replace cat with dog



(b) Replace bear with horse



(c) Replace bird with cat

Figure 11: **Visualization of Object Replacement edit.** The images above show an original image (the first one of each row) and the editing result (the other four images of each row) with different editing models. In (a), most of the results successfully replace the cat with a dog, but the result in the fourth image only replaces the head of the cat. In (b), models are required to replace the bear with the horse, the appearance is replaced successfully, though the result in the third image shows a horse with the shape of a bear's body. In (c), when trying to replace the bird with cat, most models can easily deal with the task. These results indicate that object replacement is actually an easy task for editing models, which is a natural conclusion since most editing models are trained with the object replacement instructions.



(a) Change the background of this photo to **snow**



(b) Change the background of this photo to **desert**

Figure 12: **Visualization of Background Replacement edit.** The images above show an origin image (the first one of each row) and the editing result (the other five images of each row) with different editing models. It is obvious that nearly all the models successfully complete the task, though the object in the second image in (a) is edited, we are still convinced that the model is equipped with the capability of Background Replacement, and the region editing capability will be discussed in the other dimensions.

similarly to object removal, and the whole process is designed like this:

$$\begin{aligned}
 X'_i &= Model(X_i) \\
 Machine\ Response_i &= GPT4V(Question_i, X'_i) \\
 Final\ Judgement_i &= ChatGPT(Question_i, Correct\ Answer_i, Machine\ Response_i) \\
 B_i &= \begin{cases} 1 & \text{"yes" in Final Judgement}_i \\ 0 & \text{else} \end{cases} \\
 S_{ObjectReplacement} &= \frac{1}{N_{ObjectReplacement}} \sum_{i=1}^{N_{ObjectReplacement}} B_i
 \end{aligned}$$

Background Replacement. A powerful editing model not only requires a keen perception of specific objects but also a robust ability to manipulate backgrounds effectively. For example, in Figure 12, the editing instructions "Change the background of this photo to snow" and "Change the background of this photo to desert" are provided for the editing models in (a) and (b) respectively, and the second image and the fifth image show that they fail to replace the background, which means the corresponding editing model may get a lower score in the dimension. The final judgment prompt for ChatGPT is designed here:

Question : "Is the background of this image snow? Answer Yes or No."

Correct Answer : "Yes"

Machine Response : "Yes"

Is the machine's answer correct? Answer yes or no.



(a) Change the color of the bear to **brown**



(b) Change the color of the bus to **blue**



(c) Change the color of the flowers to **purple**

Figure 13: **Visualization of Color Alteration edit.** The images above show an original image (the first one of each row) and the editing result (the other four images of each row) with different editing models. It seems that the color alteration task is not a difficult task since most of the models can get great results, but the third image in (b) edits the color of the whole image incorrectly, and the second image in (c) is only edited with few flowers. However, there's still room for editing models to improve the color alteration ability.

And we still use the LVLMs for evaluation, the scores are calculated as follows:

$$\begin{aligned}
 X'_i &= \text{Model}(X_i) \\
 \text{Machine Response}_i &= \text{GPT4V}(\text{Question}_i, X'_i) \\
 \text{Final Judgement}_i &= \text{ChatGPT}(\text{Question}_i, \text{Correct Answer}_i, \text{Machine Response}_i) \\
 B_i &= \begin{cases} 1 & \text{"yes" in Final Judgement}_i \\ 0 & \text{else} \end{cases} \\
 S_{BG\text{Replacement}} &= \frac{1}{N_{BG\text{Replacement}}} \sum_{i=1}^{N_{BG\text{Replacement}}} B_i
 \end{aligned}$$

Color Alteration. This is also a very common function for editing models. We designed an edited class including *animal, human, scenery, plant, etc.* Some results are shown in 13. The editing prompts "Change the color of the bear to brown", "Change the color of the bus to blue", and "Change the color of the flowers to purple" is used to edit the bear, bus, and flower. Then the GPT4V is used for evaluation to check if the images are correctly edited, and ChatGPT is used to get more stable results,

the ChatGPT prompt is designed below:

Question : "What color is the bus?"
 Correct Answer : "blue"
 Machine Response : "Yes"
 Is the machine's answer correct? Answer yes or no.

The whole process is designed like this:

$$\begin{aligned}
 X'_i &= Model(X_i) \\
 Machine\ Response_i &= GPT4V(Question_i, X'_i) \\
 Final\ Judgement_i &= ChatGPT(Question_i, Correct\ Answer_i, Machine\ Response_i) \\
 B_i &= \begin{cases} 1 & \text{"yes" in Final Judgement}_i \\ 0 & \text{else} \end{cases} \\
 S_{Color\ Alteration} &= \frac{1}{N_{Color\ Alteration}} \sum_{i=1}^{N_{Color\ Alteration}} B_i
 \end{aligned}$$

Style Alteration. This is a much more abstract level editing task, while the other tasks focus on editing the specific objects or background of the image. Some examples are shown in Figure 14. The style alteration task evaluates the editing models on the style understanding dimension. The CLIP model with excellent ability of abstract understanding is used for evaluation, and the CLIP scores are calculated between the images and the captions concatenated with "an image with" and the style description, "an image with cyberpunk style" for example.

$$\begin{aligned}
 X'_i &= Model(X_i) \\
 CLIP\ score_i &= CLIP(caption_i, X'_i) \\
 S_{Style\ Alteration} &= \frac{1}{N_{Style\ Alteration}} \sum_{i=1}^{N_{Style\ Alteration}} CLIP\ score_i
 \end{aligned}$$

Region Accuracy. All of the samples for evaluation in this dimension are selected from the other object-based tasks, for example, *object removal*, *object replacement*, *color alteration*. The scores are calculated with a region SSIM.

The region SSIM is designed with the mask annotated before by the Segment Anything Model(SAM). In Figure 16 showing how to use the mask on the original image and the edited image, then the scores of region accuracy can be calculated between the masked original image and the masked edited image:

$$\begin{aligned}
 X'_i &= Model(X_i) \\
 M_i &= MASK(X_i) \\
 M'_i &= MASK(X'_i) \\
 region\ score_i &= SSIM(M_i, M'_i) \\
 S_{Region\ Accuracy} &= \frac{1}{N_{Region\ Accuracy}} \sum_{i=1}^{N_{Region\ Accuracy}} region\ score_i
 \end{aligned}$$

Deblurring. This is a dimension of low-level editing, some results are shown in Figure 17, and the editing models are used to do the deblurring task with the instruction "Remove the blurriness from the image" on the deblurring dataset:

$$\begin{aligned}
 X'_i &= Model(X_i) \\
 deblurring\ score_i &= SSIM(GT_i, X'_i) \\
 S_{Deblurring} &= \frac{1}{N_{Deblurring}} \sum_{i=1}^{N_{Deblurring}} deblurring\ score_i
 \end{aligned}$$



(a) Change the image to **cyberpunk style**



(b) Change the image to **oil painting style**



(c) Change the image to **watercolor painting style**

Figure 14: **Visualization of Style Alteration edit.** The images above show an original image (the first one of each row) and the editing result (the other four images of each row) with different editing models. In (a), the image is changed to a cyberpunk style successfully, and in (b), the hotdog is changed to an oil painting style. In (c), the image is changed to a watercolor painting style, but the last result seems not that good compared with the others.

The GT in the formula is the ground truth of the deblurring dataset.

Haze Removal. This is also a low-level dimension evaluation, but it seems much easier than the deblurring task according to the experiment results in Figure 18. All of the images are clearer for human vision after the editing. The editing instruction is designed with "Remove the haze from the image" for this haze removal dimension, and the SSIM is used for evaluation:

$$\begin{aligned}
 X'_i &= Model(X_i) \\
 \text{haze removal score}_i &= SSIM(GT_i, X'_i) \\
 S_{HazeRemoval} &= \frac{1}{N_{HazeRemoval}} \sum_{i=1}^{N_{HazeRemoval}} \text{haze removal score}_i
 \end{aligned}$$

The GT in the formula is the ground truth of the haze removal dataset.

Lowlight Enhancement. This is another low-level dimension. The results in Figure 19 indicate the editing models are equipped with excellent ability on lowlight enhancement. The original images are nearly beyond the margins of human visual perception, but the edited results are effectively lightened.



(a) Change the color of the cake to blue



(b) Change the color of the flowers to purple

Figure 15: **Visualization of Region Accuracy edit.** The images above show an original image (the first one of each row), the region of editing (the second one of each row), and the editing result (the other four images of each row) with different editing models. The samples in (a) and (b) are selected from the **Color Alteration** task dataset. The results show that the edited part (inside of the mask) are correctly edited and the other part (outside of the mask) are not greatly changed.



Figure 16: The images above show an example of a region accuracy calculating process. The first image is the original image, and the third image is the editing image, here is a sample selected from **Color Alteration** dataset with the "Change the color of the bear to brown" instruction, and the second and the fourth images are masked from them respectively.

The SSIM is used for evaluation in the lowlight enhancement dimension:

$$X'_i = Model(X_i)$$

$$lowlight\ enhancement\ score_i = SSIM(GT_i, X'_i)$$

$$S_{LowlightEnhancement} = \frac{1}{N_{LowlightEnhancement}} \sum_{i=1}^{N_{LowlightEnhancement}} lowlight\ enhancement\ score_i$$

The *GT* in the formula is the ground truth of the lowlight enhancement dataset.

Noise Removal. It is a low-level dimension for evaluating the edit models. In Figure 20, the instruction "Remove the noise from the image" is used to the original image, and SSIM is used to calculate the noise removal score:



(a) Remove the blurriness from the image



(b) Remove the blurriness from the image

Figure 17: **Visualization of Deblurring edit.** The images above show an original image (the first one of each row) and the editing result (the other three images of each row) with different editing models. In (a) and (b), only the last results show the images are sharpened after editing, and the second image in (b) totally changes the original image. So the results indicate almost all the editing models are lack of the ability to deblurring.

$$\begin{aligned}
 X'_i &= Model(X_i) \\
 noise\ removal\ score_i &= SSIM(GT_i, X'_i) \\
 S_{NoiseRemoval} &= \frac{1}{N_{NoiseRemoval}} \sum_{i=1}^{N_{NoiseRemoval}} noise\ removal\ score_i
 \end{aligned}$$

The *GT* in the formula is the ground truth of the noise removal dataset.

Rain Removal. This is a low-level dimension, and the results shown in Figure 21 indicate that rain is hard to perceive. The instruction "Remove the rain from the image" is used for the task, and the SSIM is used for calculating the score:

$$\begin{aligned}
 X'_i &= Model(X_i) \\
 rain\ removal\ score_i &= SSIM(GT_i, X'_i) \\
 S_{RainRemoval} &= \frac{1}{N_{RainRemoval}} \sum_{i=1}^{N_{RainRemoval}} rain\ removal\ score_i
 \end{aligned}$$

The *GT* in the formula is the ground truth of the rain removal dataset.

Shadow Removal. This is a low-level dimension, and the results in Figure 22 show some models can complete the task perfectly. The instruction "Remove the shadow from the image" is used for the



(a) Remove the haze from the image



(b) Remove the haze from the image

Figure 18: **Visualization of Haze Removal edit.** The images above show an origin image (the first one of each row) and the editing result (the other three images of each row) with different editing models. The results in (a) and (b) show the different effects. Though the last model in (a) shows the clearest results, but it is also filled with the blue color which is abnormal. In (b), the last result shows a clear vision of the wall and food on the table, but the chair on the left is filled with black. However, the results indicate the editing is capable of doing the haze removal task to some degree.

shadow removal task, and SSIM is used for calculating the shadow removal score:

$$\begin{aligned}
 X'_i &= Model(X_i) \\
 shadow\ removal\ score_i &= SSIM(GT_i, X'_i) \\
 S_{ShadowRemoval} &= \frac{1}{N_{ShadowRemoval}} \sum_{i=1}^{N_{ShadowRemoval}} shadow\ removal\ score_i
 \end{aligned}$$

The GT in the formula is the ground truth of the shadow removal dataset.

Snow Removal. This is a low-level dimension, and the results in Figure 23 show some models can remove the snow as expected, but most models can not. The instruction "Remove the snow from the image" is used for the snow removal task, and SSIM is used for calculating the snow removal score:

$$\begin{aligned}
 X'_i &= Model(X_i) \\
 snow\ removal\ score_i &= SSIM(GT_i, X'_i) \\
 S_{SnowRemoval} &= \frac{1}{N_{SnowRemoval}} \sum_{i=1}^{N_{SnowRemoval}} snow\ removal\ score_i
 \end{aligned}$$

The GT in the formula is the ground truth of the snow removal dataset.

Watermark Removal. This is a low-level dimension, and the results in Figure 24 show some models can remove the watermark perfectly or fade out the watermark to some degree. The instruction "Remove the watermark from the image" is used for the watermark removal task, and SSIM is used



(a) Enhance the brightness of an image



(b) Enhance the brightness of an image

Figure 19: **Visualization of Lowlight Enhancement edit.** The images above show an origin image (the first one of each row) and the editing result (the other three images of each row) with different editing models. The results in (a) and (b) show the editing models are good at copying with the low light task. Nearly all of the models can lighten the images successfully.

for calculating the snow watermark score:

$$X'_i = Model(X_i)$$

$$watermark\ removal\ score_i = SSIM(GT_i, X'_i)$$

$$S_{WatermarkRemoval} = \frac{1}{N_{WatermarkRemoval}} \sum_{i=1}^{N_{WatermarkRemoval}} watermark\ removal\ score_i$$

The GT in the formula is the ground truth of the watermark removal dataset.

A.2 More Details on Data Annotation.

Counting. The counting evaluation dimension aims to assess the model’s ability to accurately comprehend quantity-related instructions and precisely modify images accordingly. To conduct this evaluation, we manually curated a set of 136 photos from the widely used MS-COCO dataset. Subsequently, we annotated textual editing instructions for each image, based on the content depicted. To promote diversity in the editing instructions, we employed ChatGPT, as illustrated in Fig. 25. We utilized ChatGPT to modify the original instructions into varied alternatives. Specifically, we formulated a prompt for ChatGPT, which was structured as follows: "Please provide a different expression for the following sentence: *<original instruction>*". Besides, for each sample in the high-level editing dimension, we annotate a category, such as animal, object, scenery, plant, human, For instance, in Fig. 26 (right), we present an image featuring a man capturing a photograph of a snowy mountain. The original instruction assigned to this image was "Add eight birds to the image", and the ChatGPT-enhanced diverse instruction became "Decorate the image with a group of eight birds".

Direction Perception. The dimension of direction perception aims to assess the editing model’s capability to accurately comprehend positional descriptions in instructions and execute corresponding



(a) Remove the noise from the image



(b) Remove the noise from the image

Figure 20: **Visualization of Noise Removal edit.** The images above show an original image (the first one of each row) and the editing result (the other three images of each row) with different editing models. In (a), the second image removes the noise but changes too much, and the other results seem changed a little. In (b), the second and the last images also changed too much and the third one seems smoother. The results indicate the editing models are not good at dealing with the noise.

image modifications. We selected 139 images from the MS-COCO dataset and annotated them accordingly. Illustrated in Fig. 27(left), the chosen image portrays a group of people arranging cakes on a desk. The original instruction, annotated by human annotators, states, "Add a dog to the top of the desk," while the diverse instruction refined by ChatGPT is, "Position a dog atop the desk."

Object Removal. The Object Removal dimension evaluates the ability of the editing model to accurately eliminate the target object from the image based on the provided instructions. We carefully curated a set of 139 images from the MS-COCO dataset and meticulously annotated them accordingly. For instance, as depicted in Fig. 28 (left), we show a picture of a man surfing. The original instruction for this picture is "Remove the man from the image", while ChatGPT's enhanced diversification instruction becomes "Delete the man from the picture".

Object Replacement. The objective of the object replacement dimension is to substitute an object in the image with another object based on the provided instruction. We meticulously curated a set of 136 images from the MS-COCO dataset and annotated them with utmost care. As illustrated in Fig. 29 (right), the selected image shows two zebras on the grass. The original instruction given by the human annotator is "replace zebra with child", while the diversified instruction after optimization by ChatGPT is "Replace the zebra with an energetic child".

Background Replacement. Aside from editing foreground objects, modifying the background is also a crucial evaluation dimension for the editing model. Therefore, the Background Replacement dimension focuses on altering the image's background according to the provided textual instructions. With meticulous curation, we assembled a set of 139 images from the MS-COCO dataset and annotated them meticulously. For instance, as depicted in Fig. 30 (right), we present an image featuring a man cooking in the kitchen. The original instruction for this image is "Change the background of this photo to snow", while ChatGPT's enhanced diversification instruction becomes "Rearrange the elements in this picture to simulate a snowy backdrop".



(a) Remove the rain from the image



(b) Remove the rain from the image

Figure 21: **Visualization of Rain Removal edit.** The images above show an original image (the first one of each row) and the editing result (the other three images of each row) with different editing models. In (a), the rain is not removed in the second and the fourth image, and the car in the second image is influenced. The rain in the third image is removed but the image is changed. In (b), the third image is also over-edited, and the third image fails to remove the rain, only the last result makes the color lighter to remove the rain to some degree.

Color Alteration. Color Alteration involves modifying object attributes. This dimension aims to assess the model’s ability to accurately change the color of the target object based on the provided instructions. Through careful curation, we compiled a set of 138 images from the MS-COCO dataset, subjecting them to meticulous instruction annotation. For instance, as depicted in Fig. 31 (left), we display an image featuring a person skiing. The original instruction associated with this image is "Change the color of the ground to brown", while the enhanced and diversified instruction provided by ChatGPT becomes "Brown the ground’s color".

Style Alteration. Style transfer is a crucial task in computer vision that entails creating a novel image by merging the content of one image with the style of another. It is also reasonable to consider utilizing textual instructions to alter the style of an image. The Style Alteration dimension endeavors to evaluate the editing model’s ability to modify an image’s style. We meticulously curated a set of 140 images from the MS-COCO dataset and subjected them to detailed annotation. This evaluation is illustrated in Fig. 32 (left). The selected image depicts an urban street scene at night. The original instruction provided by the human annotator is "Change the image to cyberpunk style," while the diversified instruction refined by ChatGPT reads, "Transform the image into a futuristic and gritty cyberpunk dystopia."

Region Accuracy. In the task of instruction-based image editing, our focus extends beyond the accuracy of editing the target object; we also consider the preservation of non-target objects. To assess the level of retention of these non-target objects, we introduce the Region Accuracy dimension. To facilitate this evaluation, we select 140 images and their corresponding annotations from the Object Removal, Object Replacement, and Color Alteration dimensions. Additionally, we manually annotate the masks for the edited objects by following the provided instructions. For instance, as



(a) Remove the shadow from the image



(b) Remove the shadow from the image

Figure 22: **Visualization of Shadow Removal edit.** The images above show an original image (the first one of each row) and the editing result (the other three images of each row) with different editing models. In (a), the second image adds a human to the image incorrectly, the third image fails to remove the shadow, while the last one successfully removes it. In (b), the second image seems to be changed into a black-and-white image, and the last image seems to enhance the shadow erroneously. The third image shows a perfect result on shadow removal, and not damaging the road structure.

depicted in Fig. 33, the original instruction is "Change the color of the clothes on the man to red", so we annotate the mask to encompass only the clothes of the man.

Deblurring. The Deblurring dimension is designed to assess the model’s ability to remove image blurring and enhance clarity. We collect a set of 140 blurred and deblurred images from the deblurring datasets, specifically GoPro Nah et al. [2017] and HIDE Shen et al. [2019]. The original instruction provided for all images is "Remove the blurriness from the image." To introduce diversity in the instructions, we employ ChatGPT, resulting in distinct instructions for each image, such as "Enhance the clarity of the image," "Clear up the blur in the picture," "Sharpen the image to remove blurriness," and so on. In the low-level editing dimension, we annotate each sample’s category as "global." Fig. 34 illustrates the process. First, we obtain the input image and ground-truth image from the publicly available deblurring dataset. Next, we manually annotate the image with the original instruction, "Remove the blurriness from the image". Finally, we obtain diverse instructions, such as "Sharpen the image to remove blurriness" using ChatGPT.

Haze Removal. The Haze Removal dimension focuses on assessing the model’s capability to eliminate haze from images. To create the evaluation dataset, we initially collect a total of 155 input images and corresponding ground-truth images from the Dense-Haze Ancuti et al. [2019] and Haze4k Liu et al. [2021b] datasets. As shown in Fig. 35, we initially acquire the input image and the real image from the de-hazing dataset. Then, we manually label the image with the original instruction, "Remove the haze from the image." Finally, utilizing ChatGPT, we generate diverse instructions, such as "Eliminate the mist in the picture."

Lowlight Enhancement. The Lowlight Enhancement dimension focuses on evaluating the model’s ability to improve image brightness, thereby enhancing image clarity. For this evaluation, we select a set of 140 input images and their corresponding ground-truth images from the LOL dataset Wei et al.



(a) Remove the snow from the image



(b) Remove the snow from the image

Figure 23: **Visualization of Snow Removal edit.** The images above show an original image (the first one of each row) and the editing result (the other three images of each row) with different editing models. In (a), the second image replaces the snow with a cloud, but the buildings are over-changed, the third image removes part of the snow, and the last image replaces the snow with the blue sky, the buildings are much clearer. In (b), the second image successfully removes most of the snow while the others fail.

[2018]. As shown in Fig. 36, we obtain input images and real images from the lowlight enhancement datasets. Then, we manually annotate the images with the original instruction: "Enhance the brightness of an image". Subsequently, we utilize ChatGPT to generate diverse instructions, such as "Boosting the luminosity".

Noise Removal. The Noise Removal dimension focuses on evaluating the model's ability to successfully eliminate noise from images. To conduct this evaluation, we collect a set of 120 input images and their corresponding ground-truth images. We obtain these images by sampling from the CBSD68 dataset [Martin et al. \[2001\]](#) and adding noise to sampled images from the MS-COCO dataset. In addition, we gather both original instructions and diverse instructions from both human annotators and ChatGPT. As shown in Fig. 37, We first acquire input images and ground truth images from the denoising image datasets. Next, we manually annotate the images with the original instruction: "Remove the noise from the image." Finally, we utilize ChatGPT to generate diverse instructions like "Cleanse the image from visual interference through noise removal."

Rain Removal. The Rain Removal dimension aims to assess the model's capability to effectively remove rain from images. For this evaluation, we collect a dataset consisting of 140 input images and their corresponding ground-truth images sampled from the LHP-Rain dataset [Guo et al. \[2023b\]](#). Fig. 38 illustrates the dataset used for this dimension. We initially obtained the input image and the real image from the rain removal dataset. Following the original instruction, we manually annotate the image to "Remove the rain from the image." Later, we utilize ChatGPT to generate diverse instructions, including "Extract the rain from the scene."

Shadow Removal. The Noise Shadow dimension evaluates the model's effectiveness in removing shadows from images. To conduct this assessment, we gather a dataset comprising 140 input images and their corresponding ground-truth images sampled from the SRD dataset [Qu et al. \[2017\]](#). Fig. 39



(a) Remove the watermark from the image



(b) Remove the watermark from the image

Figure 24: **Visualization of Watermark Removal edit.** The images above show an original image (the first one of each row) and the editing result (the other three images of each row) with different editing models. In (a), the watermark can be removed at different percentages, but the last image removes everything except the watermark. In (b), the second image shows a perfect result, but the third image changes the whole image into the watermark style, and the last image adds another new watermark to the image by mistake.

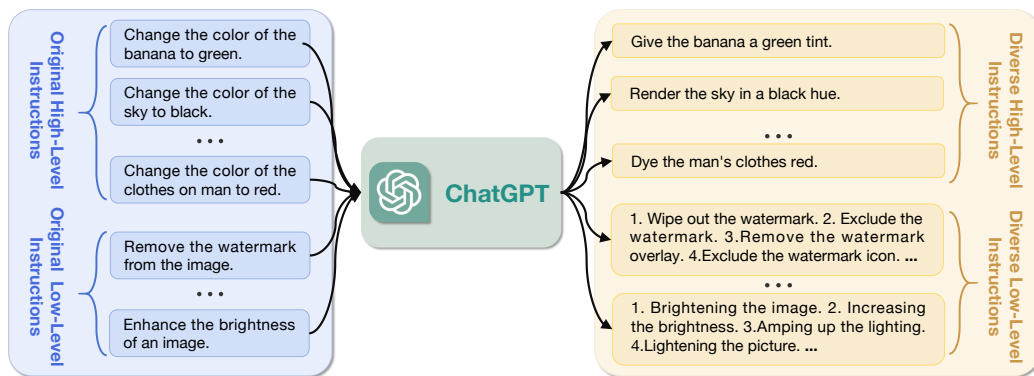


Figure 25: Convert original instructions to reverse instructions using ChatGPT.



Original Instruction: Add a dog to the image

Diverse Instruction: Introduce a dog presence into the picture



Original Instruction: Add eight birds to the image

Diverse Instruction: Decorate the image with a gathering of eight birds

Figure 26: Visualization of the selected images, original instructions, and diverse instructions of the counting dimension.



Original Instruction: Add a dog to the top of the desk

Diverse Instruction: Position a dog atop the desk



Original Instruction: Add a tiger to the left of the giraffe

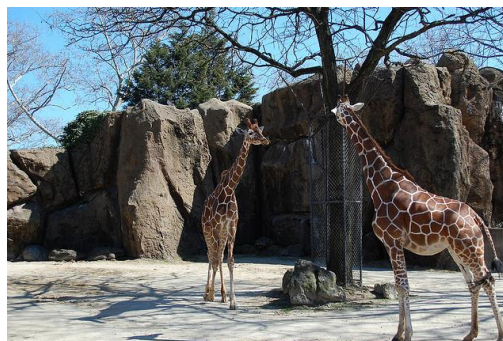
Diverse Instruction: Affix a majestic tiger to the left side of the giraffe

Figure 27: Visualization of the selected images, original instructions, and diverse instructions of the Direction Perception dimension.



Original Instruction: Remove the man from the image

Diverse Instruction: Delete the man from the picture



Original Instruction: Remove the giraffes from the image

Diverse Instruction: Get rid of the giraffes in the picture

Figure 28: Visualization of the selected images, original instructions, and diverse instructions of the object removal dimension.



Original Instruction: replace woman with dog

Diverse Instruction: Replace the woman with a loyal dog



Original Instruction: replace zebra with child

Diverse Instruction: Replace the zebra with an energetic child

Figure 29: Visualization of the selected images, original instructions, and diverse instructions of the object replacement dimension.



Original Instruction: Change the background of this photo to snow

Diverse Instruction: Adjust the setting of this image to reflect a snowy landscape



Original Instruction: Change the background of this photo to snow

Diverse Instruction: Rearrange the elements in this picture to simulate a snowy backdrop

Figure 30: Visualization of the selected images, original instructions, and diverse instructions of the background replacement dimension.

visually represents the dataset utilized for this dimension. First, we acquire input images along with their corresponding ground truth images from the shadow removal dataset. Next, we manually label these images according to the core instruction, which reads, "Remove the shadow from the image". Then, we leverage ChatGPT to generate alternative instructions like " Erase the shadow cast in the image".

Snow Removal. The objective of Snow Removal is to efficiently minimize or eliminate snow from images. For our study, we carefully chose 140 images from the CSD dataset [Chen et al. \[2021\]](#) and performed the necessary annotations. As shown in Fig. 40, firstly, we obtain the input image and the real image from the snow removal dataset. Then, we manually annotate the image with the original instruction "Remove the snow from the image". Finally, we acquire diverse instructions through ChatGPT, for instance, "Delete the snow from the image."

Watermark Removal. The Watermark Removal dimension aims to evaluate the model's ability to effectively remove watermarks from images. For this evaluation, we compile a dataset consisting of 140 input images and their corresponding ground-truth images sampled from the CLWD dataset [Liu et al. \[2021a\]](#). Fig. 41 provides a visual representation of the dataset used for this dimension. After obtaining the input image and the real image from the watermark-free dataset, we manually label



Original Instruction: Change the color of the ground to brown

Diverse Instruction: Brown the ground's color



Original Instruction: Change the color of the sea surface to green

Diverse Instruction: The sea surface shall turn green

Figure 31: Visualization of the selected images, original instructions, and diverse instructions of the color alteration dimension.



Original Instruction: Change the image to cyberpunk style

Diverse Instruction: Transport the image into a futuristic and gritty cyberpunk dystopia



Original Instruction: Change the image to oil painting style

Diverse Instruction: Capture the essence of the scene with the depth and richness of oil painting

Figure 32: Visualization of the selected images, original instructions, and diverse instructions of the style alteration dimension.

Input Image



Annotated Mask



Original Instruction: Change the color of the clothes on man to red

Diverse Instruction: Dye the man's clothes red

Figure 33: Visualization of the selected images, original instructions, and diverse instructions of the Region Accuracy dimension.

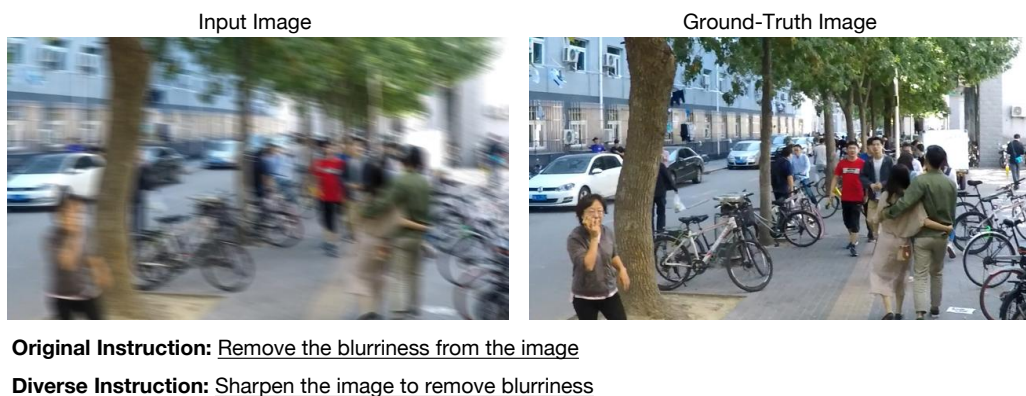


Figure 34: Visualization of the selected images, original instructions, and diverse instructions of the Deblurring dimension.

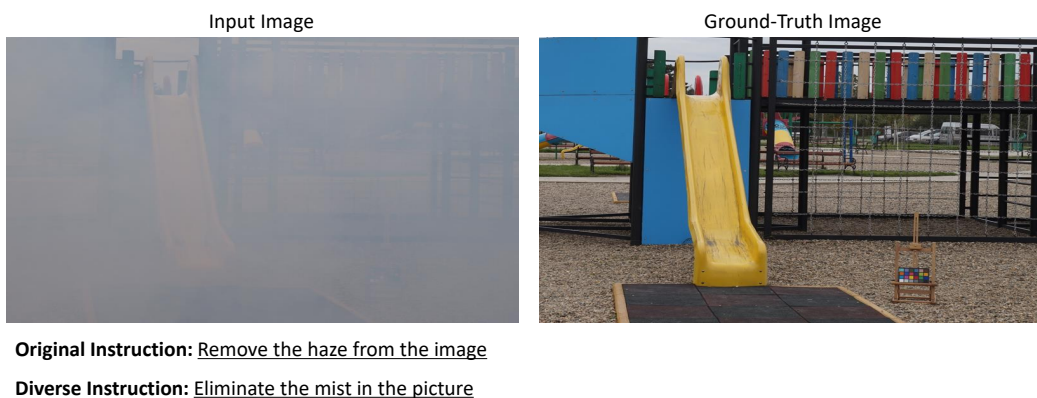


Figure 35: Visualization of the selected images, original instructions, and diverse instructions of the Haze Removal dimension.

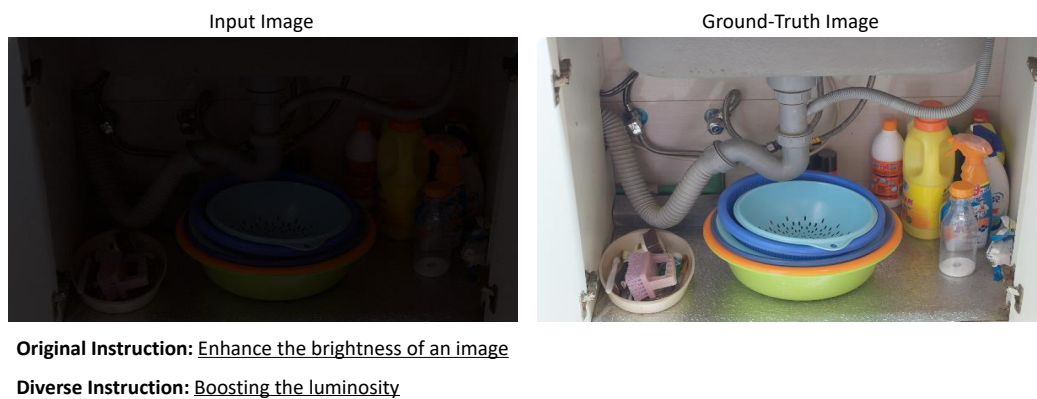
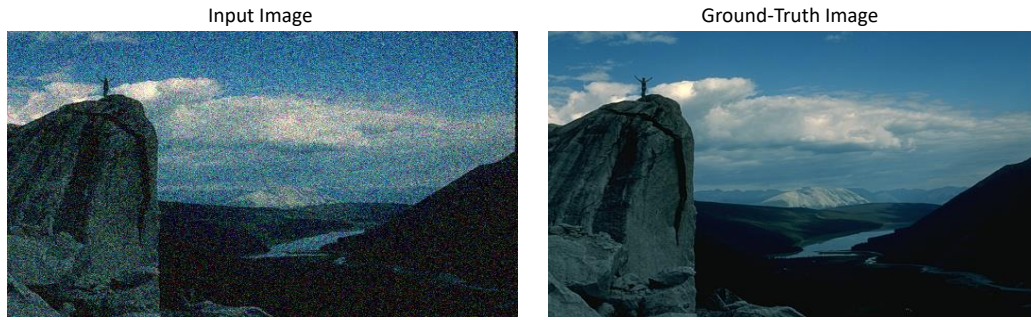


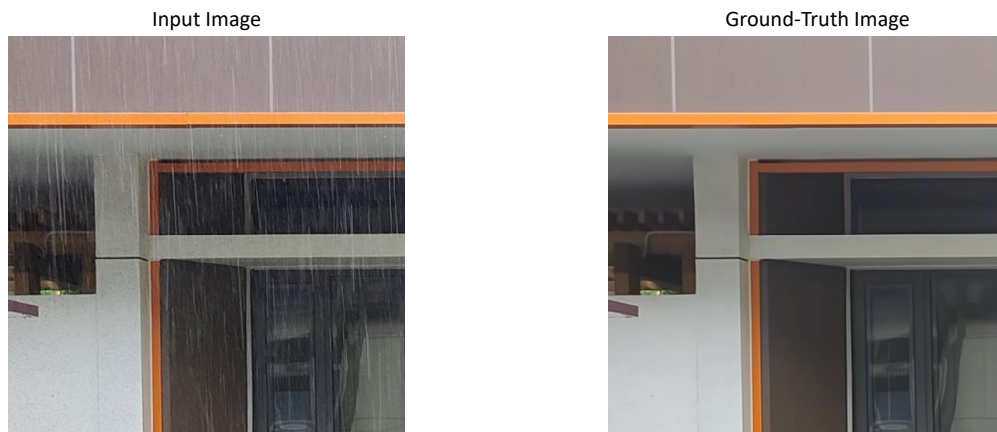
Figure 36: Visualization of the selected images, original instructions, and diverse instructions of the Lowlight Enhancement dimension.



Original Instruction: Remove the noise from the image

Diverse Instruction: Cleanse the image from visual interference through noise removal

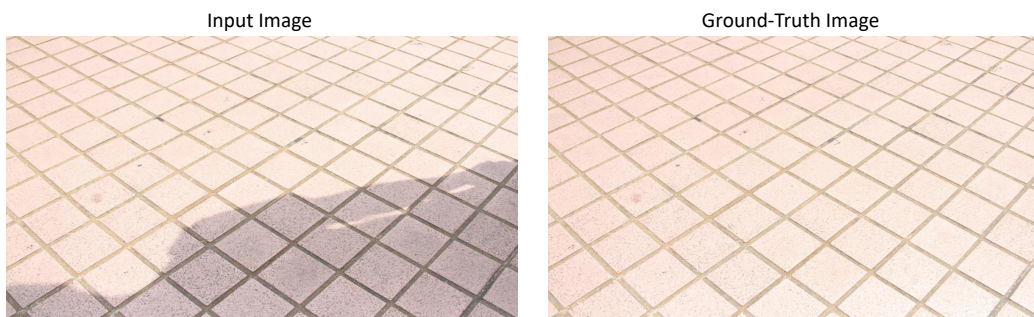
Figure 37: Visualization of the selected images, original instructions, and diverse instructions of the Noise Removal dimension.



Original Instruction: Remove the rain from the image

Diverse Instruction: Extract the rain from the scene

Figure 38: Visualization of the selected images, original instructions, and diverse instructions of the Rain Removal dimension.



Original Instruction: Remove the shadow from the image

Diverse Instruction: Erase the shadow cast in the image

Figure 39: Visualization of the selected images, original instructions, and diverse instructions of the Shadow Removal dimension.

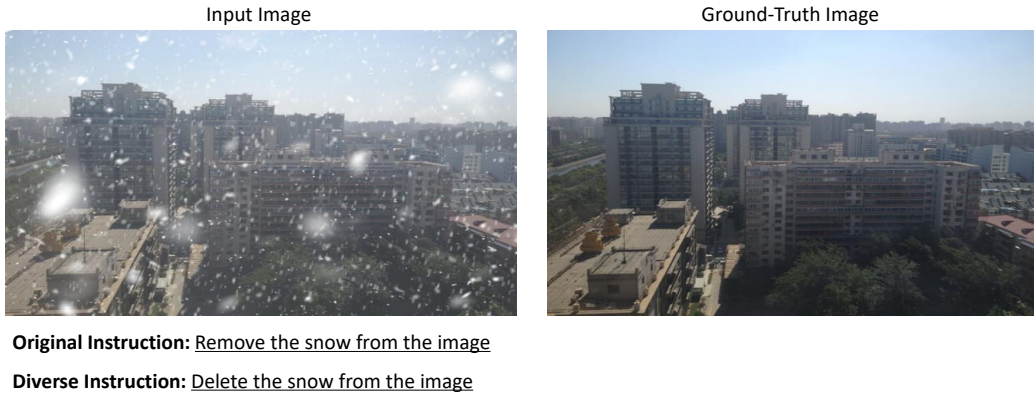


Figure 40: Visualization of the selected images, original instructions, and diverse instructions of the Snow Removal dimension.



Figure 41: Visualization of the selected images, original instructions, and diverse instructions of the Watermark Removal dimension.

the image with the original instruction "Remove the watermark from the image". Then, we used ChatGPT to obtain various instructions like "Exclude the watermark".